Stability Study of Ormo Tower

Master of Science Thesis in Geo and Water Engineering

SILESHI MEKONNEN TIRUNEH

Department of Civil and Environmental Engineering
Division of Geo Engineering
Geotechnical Engineering Research Group
CHALMERS UNIVERSITY OF TECHNOLOGY
Göteborg, Sweden 2010

Master's Thesis 2010:01

MASTER'S THESIS 2010:01

Stability Study of Ormo Tower

Master's Thesis in the International Master's Programme *Geo and Water Engineering*

SILESHI MEKONNEN TIRUNEH

SUPERVISORS:

Andreas Åberg and Peter Wilén, Vattenfall Power Consult AB

Claes Alén, Chalmers University of Technology

Department of Civil and Environmental Engineering
Division of Geo Engineering
Geotechnical Engineering Research Group
CHALMERS UNIVERSITY OF TECHNOLOGY
Göteborg, Sweden 2010

Stability Study of Ormo Tower
Master's Thesis in the International Master's Programme *Geo and Water Engineering*
SILESHI MEKONNEN TIRUNEH

Master's Thesis 2010:01
Department of Civil and Environmental Engineering
Division of Geo *Engineering*
Geotechnical Engineering Research Group
Chalmers University of Technology
SE-412 96 Göteborg
Sweden
Telephone: + 46 (0)31-772 1000

Cover:
Ormo Towers, Photo Vattenfall.

Chalmers Reproservice/ Department of Civil and Environmental Engineering
Göteborg, Sweden 2010

Stability Study of Ormo Tower
Master's Thesis in the international Master's Programme *Geo and Water Engineering*
SILESHI MEKONNEN TIRUNEH
Department of Civil and Environmental Engineering
Division of Geo Engineering
Geotechnical Engineering Research Group
Chalmers University of Technology

ABSTRACT

Any civil Engineering structure can be subjected to unanticipated loads during the design life of the structure. These loads can be resulted from natural phenomena or manmade impacts. In any case, it is very important to check the stability to insure the safety or to take remedy action so that catastrophic failure can be avoided.

Ormo tower which is located in the Nordre River, on the south- west cost of Sweden, is an important structure which is responsible for the prevention of intrusion of sea water into the water production plant. This function makes the tower very important as the city of Gothenburg and the neighbouring towns relay on Gota River for their supply of clean water. The tower has been subjected to lateral load from the newly built embankment and increasing wind load which result from the change in climate.

The initial work deals about the geotechnical investigation of the site. This was done by analysing the CPT tests made on the nearby area by Banverket (Swedish rail road Administration). A literature study was also been made on the type of material used for the embankment and the foundation.

The characteristic load on the structure and the corresponding design load is calculated using partial factor of safety. The design resistance capacity of the soil is also calculated from the data obtained from the boreholes around the tower.

Finally, the stability analysis of the tower is made according to limit state method and the values are computed using Geosuite pile group and hand calculation. The result obtained can be used for further studies and decision making purpose by Vattenfall Power Consult AB.

Key words: Lateral earth pressure, wind load, Pile foundation, undrained shear strength, pile-soil interaction, ultimate limit state design, serviceability limit state design.

Contents

Preface

This Master thesis project has been carried out at Chalmers University of Technology, in the department of Civil and Environmental Engineering, division of Geo Engineering and in cooperation with Infrastructure and Civil Engineering department of Vattenfall Power Consultant AB. The project has been initiated by Mr Andreas Åberg and Mr Peter Wilén from Vattenfall Power Consultant AB.

Ormo tower, which is located at the northern outflow to the sea of Göta River, which is also called Nordre river, has been subjected to lateral pressure from a newly built embankment and wind load and its stability is a concern for Vattenfall.

In this project the stability of Ormo tower has been investigated for both serviceability and ultimate limit states. In the Geotechnical investigation part, the site investigation undertaken by Swedpower is used moreover, in the analysis part, the soil model developed by NTNU is applied while performing calculation using Geosuite Pile Group. Finally, the results and the conclusion drawn is presented, which can be used for decision making purpose by Vattenfall.

Göteborg February 2010

Sileshi Mekonnen Tiruneh

Acknowledgements

I would like to express my deepest gratitude to my teacher, Professor Claes Al**é**n at the department of Civil and Environmental Engineering for his help in providing valuable information. I have also gained a lot of knowledge in all the courses that I took with him.

I also want to thank Mr Andreas Åberg and Mr Peter Wilén for initiating this master thesis and accepting me to work on it, particularly Mr Andreas Åberg has been supervising and giving me feedback during the course of the work. I want to thank him for his effort in providing very useful information.

Last, but not least, I am indebted to my family especially my father and my mother who has been supporting and encouraging me to fulfill my dream.

Notations

Roman upper case letters

A^*	A constant which depends on the angle of friction
A_i	Projected area of the tower perpendicular to the wind direction
C_e	Exposure coefficient
C_{pe}	External pressure coefficient
C_{pi}	Internal pressure coefficient
C_o	Orography factor
$E_{new,k}$	Characteristic value of soil earth pressure in kN, for 3D earth pressure distribution
$E_{new,kB}$	Characteristic value of soil earth pressure in kN, for 3D earth pressure distribution Case B
$E_{new,kC}$	Characteristic value of soil earth pressure in kN, for 3D earth pressure distribution Case C
$E_{new,d,B}$	Design value of earth pressure in KN, for 3D earth pressure distribution in Case B
$E_{new,d,C}$	Design value of earth pressure in KN, for 3D earth pressure distribution in Case C
F	Total lateral force
F_{wk}	The characteristic value of wind force acting at length X_i from the ground
F_{wdB}	The design value of wind force for Case B
F_{wdC}	The design value of wind force for Case C
$F_{water,k}$	The characteristic value of the force on the screen wall due to the water
$F_{water,dB}$	The design value of the force on the screen wall due to the water for Case B
$F_{water,dC}$	The design value of the force on the screen wall due to the water for Case C
H	Total height of the tower
K_a	Rankine earth pressure coefficient
K_{adB}	Design value of Rankine earth pressure coefficient for Case B
K_{adC}	Design value of Rankine earth pressure coefficient for Case C
K_r	Roughness factor
L	Width of tower
L_{new}	Modified width of the tower for 3D earth pressure distribution
M	Bending moment at the pile cap
M_{dx}	Factored bending moment in the X direction
M_{dy}	Factored bending moment in the Y direction
P_a	Lateral earth pressure in kPa for 2D earth pressure distribution
P_{akB}	Lateral earth pressure in kPa for 2D earth pressure distribution for Case B
P_{akC}	Lateral earth pressure in kPa for 2D earth pressure distribution for Case C
$P_{d\max}$	Design value of maximum axial load on a single pile
$P_{w,downstream}$	Water pressure on the screen at the downstream side

$P_{w,upstream}$	Water pressure on the screen at the upstream side
$P_{w,net}$	Net water pressure
V_b	Basic wind velocity
V_{bnew}	Basic wind velocity when climate change considered
W_e	External wind pressure
W_i	Internal wind pressure
W_{ei}	External wind pressure between upper and lower parts of the tower
W_{el}	External wind pressure at lower part of the tower
W_{eu}	External wind pressure at upper parts of the tower
X_i	Arm length
X_k	Characteristic value of a strength property for timber
X_d	Design value of a strength property for timber
Z	Height from ground level
Z_e	Height from ground level for external surface
Z_i	Height from ground level for internal surface

Roman lower case letters

d_x	Distance in the Y direction from centre of gravity of pile group to pile for which $P_{\max}$ is being calculated
d_y	Distance in the Y direction from centre of gravity of pile group to pile for which $P_{\max}$ is being calculated
h_{strip}	Strip of height used for the calculation of peak velocity pressure
Δh	The water level difference
h_1	Depth of water at the upstream
h_2	Depth of water at the downstream
k_{mod}	Modification factor taking into account the effect of the duration of load and moisture
l_{screen}	Length of screen wall
n	Number of piles
q_b	Basic velocity pressure
q_p	Peak velocity pressure
q_{pl}	Peak velocity pressure at the lower part of the tower
q_{pi}	Peak velocity pressure between the upper and lower part of the tower
q_{pu}	Peak velocity pressure at the upper part of the tower

Greek lower case letters

ρ	Air density
γ	Total unit weight of backfill
γ'	Effective unit weight of the backfill
γ_w	The unit weight of water
ϕ	Angle of internal friction of the backfill material

ϕ_{dB}	Design value of angle of internal friction of the backfill material for Case B
ϕ_{dC}	Design value of angle of internal friction of the backfill material for Case C
$\delta_{h,a}$	Lateral displacement of the wall
β	Inclination of the backfill material from the horizontal
γ_{GB}	Partial safety factor for permanent action, Case B
γ_{GC}	Partial safety factor for permanent action, Case C
γ_{QB}	Partial safety factor for variable action, Case B
$\gamma_{\tan\phi' B}$	Partial safety factor for shearing resistance, Case B
γ_{cuB}	Partial safety factor for Undrained shear strength, Case B
γ_{QC}	Partial safety factor for variable action, Case C
$\gamma_{\tan\phi' C}$	Partial safety factor for shearing resistance, Case C
γ_{cuC}	Partial safety factor for Undrained shear strength, Case C
γ_{M}	Partial factor for a material property

1 INTRODUCTION

Water barrier structures have been built for a long time in history. In the past the main purposes of these structures were to accumulate water, which is abundant in the rainy season so that it can be used in the dry season, much of it being for drinking water and irrigation.

The subsequent transformation of societies from pre-industrial to industrial ones resulted in the use of water barrier structures for different purposes like for hydropower generation, water supply, flood control, ground water recharging etc. Apart from these major uses there are also several applications of these structures which basically arise from the increased knowledge of the environment and the need to increase the quality of life.

One such use, which is the focus of this paper, is the prevention of intrusion of seawater in to Göta River, which is used for production of fresh water in Gothenburg and the neighboring towns. Figure 1.1 Shows map of Sweden and the city of Gothenburg.

Figure 1.1 Map of Sweden

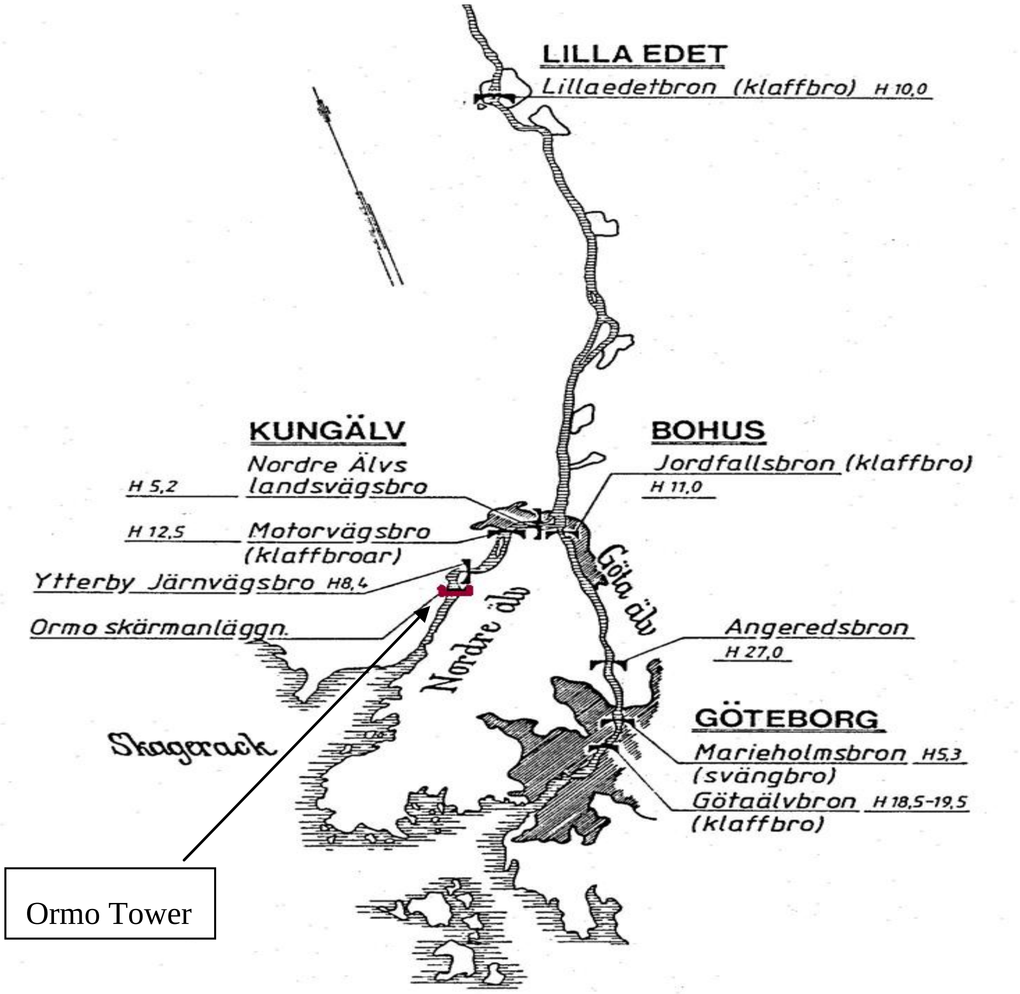

Figure 1.2 Site map of Ormo Screen Plant

Göta River is a river that drains Lake Vänern in to Kattegatt at the city of Gothenburg, on the west coast of Sweden. As shown in the above figure at Kungälv town, the river splits into two, with the northern part being the Nordre River and the southern part keeping the same name Göta River, the fresh water intake for Gothenburg is located some kilometres downstream of the south branch. At Trollhättan and Lilla Edet, downstream of Lake Vänern, there are dams for hydropower purpose and the dams regulate the flow of Göta River. If the flow of water in the Göta River is very low, back flow of water from Skagerack Sea, to both branches of Göta River is inevitable. This back flow of sea water into Göta River has a big impact on the water supply system. To avoid this problem the flow of water in the southern branch should be increase. During period of low flow, to maintain a higher flow in the Göta River, the flow in the Nordre River should be restricted. Hence, as located in the Figure below, screen (Regulating) structure is constructed on Nordre River, to avoid the intrusion of salt water in to the fresh water production plant.

Ormo screen has two towers, which house machineries to maneuver four screens that restrict the flow of Nordre River. The system works by the ropes/wires attached to the counterweight and the counterweight is filled with varying amount of water to balance the variable water pressure on the screen (Forsberg et. al, 2002).

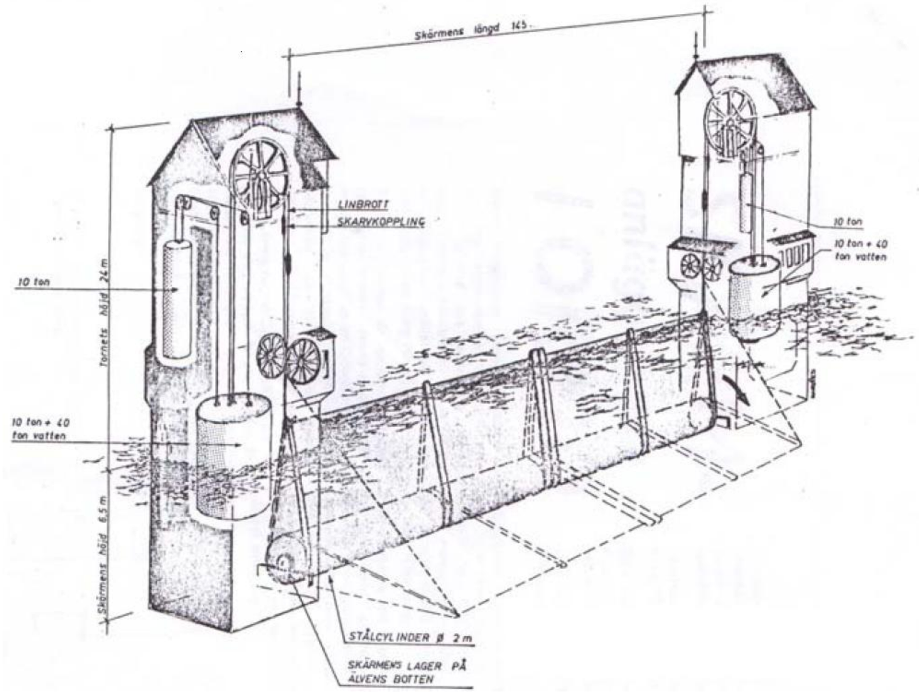

Figure 1.3 Three Dimensional view of Ormo Screen plant

The structure is equipped with a mechanical system, which operates remotely, either to open or to close the screen so as not to let the seawater mix in to the river. The structure is mainly important in summer time, when river discharge is low and sea level is high. The intrusion of seawater in winter is less crucial due to the high discharge of the river and low sea level.

1.1 Background and Scope

This Master Thesis deals with the stability problem, which might encounter at Ormo tower. The purpose of the tower, as said above is to control the flow of Nordre River and thus indirectly the flow of Gota River. By doing this it controls the intrusion of salt to the water intake from Göta River.

The plant was built in the 1930's and has been restored in two stages, one in 1950's and the other in 1970's. Stability condition for the left tower has been studied and some measurements and checks have been performed. Under normal circumstances, the stability is not a problem. The climate changes in the future might result in increased wind load, which will be added to the earth pressure from the embankment, to exert a higher lateral load to the tower. In addition to the pressure from the embankment, there is also a horizontal pressure from the water, which is perpendicular to the pressure from the embankment. The effects of all these loads on the stability of the tower which should be studied to guarantee, the plant's continued operation in the longer term.

Ormo screen is provisionally classified as a Class A plant, which means that the impact on social functioning due to loss of function of the system would be great (Forsberg et. al, 2002).

1.2 Outline

The study is basically divided into four different parts as presented in the chapters below. Chapter 2 presents the Geotechnical studies in the area followed by chapter 3, which deals with Geometry of the Structure, Foundation material and Loading direction. In part 4 calculations of action forces namely wind load, earth pressure and water pressure has been performed.

In the stability calculation, chapter 5, the action forces are applied on the structure to find out if reaction is greater than the action or if the deflection of the structure is within the permissible limit. To do this a simplification of the actual condition was necessary and hence a conceptual model for performing the analysis has also been discussed. The calculation is performed using the software called Geosuite pile group. The stability analysis is performed for ultimate limit state and serviceability limit state.

Finally the compilation of results and assessments are presented in Chapter 6.

2 Geotechnical Investigation

The geotechnical investigation undertaken in this study doesn't involve any kind of laboratory testing nor in situ testing specifically for this project; it is merely concentrated on a desk study of previous reports and site visits.

2.1 Site Visit

The purpose of the site visit was to study the topography of the site, the condition of the embankment and the tower itself. There were two separate site visits the first one was just to observe the general view of the ground around the tower and the nearby facilities (the rail road and a gas pipe line). The second one was a closer view of the east side of the tower where the stability problem is a concern. In this visit we were able to observe the settlement of the newly built embankment. The settlement increases as we go to the shoreline of the river. This is indirect contrast to our expectation since the weight of the embankment is larger at the tower and thus we expected more settlement near the tower. This probably is due to the softening of the riverside by erosion (hydraulic action), which resulted in consolidation of the clay beneath the original embankment.

2.2 Desk Study

The desk study is based on the site investigation undertaken by Swedpower and Banverket (Swedish Rail administration) when they build the nearby gas pipeline and railroad respectively. These two facilities are located very close to the tower and it is assumed that the data obtained fairly represent the soil condition near the tower.

2.2.1 Soil Condition

The soil condition was investigated using different methods, which include vane shear test, piston sampling, CPT (Cone Penetration Test) and seismic method. The area around the Nordre River, constitute mainly of clay with varying depth. Generally the depth of the clay increases as we approach the riverside.

The shear strength has been measured at several locations[1]. The result obtained by Swedpower is 10 kPa which increases by 1 kPa/m by depth. On the other hand VBB Viak (another consultant firm hired by Banverket) did an investigation and found out that the shear strength at the ground level is 8 kPa, which increases by 1.2 kPa/m[2] by depth. The site map, where the site investigation carried out can be seen in appendix I and appendix II (SwedPower).

---

[1] This measurement is made on a very large area, but the shear strength used in this report is from the bore holes near the tower and it is shown in section 5.2.

[2] According to the result from the three bore holes the increase in Undrained shear strength is 1.7 kPa/m

At the river side, the soil is exposed to lower effective stresses due to the water level in the river and, therefore, has a lower shear strength, which approximately equal to 8 kPa at the uppermost layer and an increases of 1.2 kPa/m downwards.

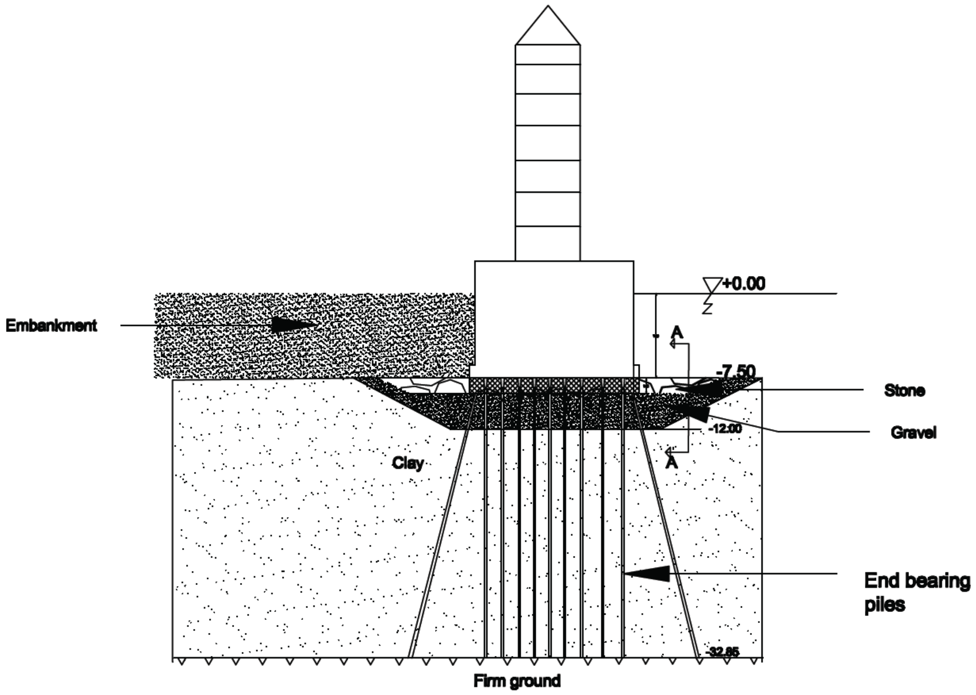

Figure 2.1 The cross sectional dimension of the Tower

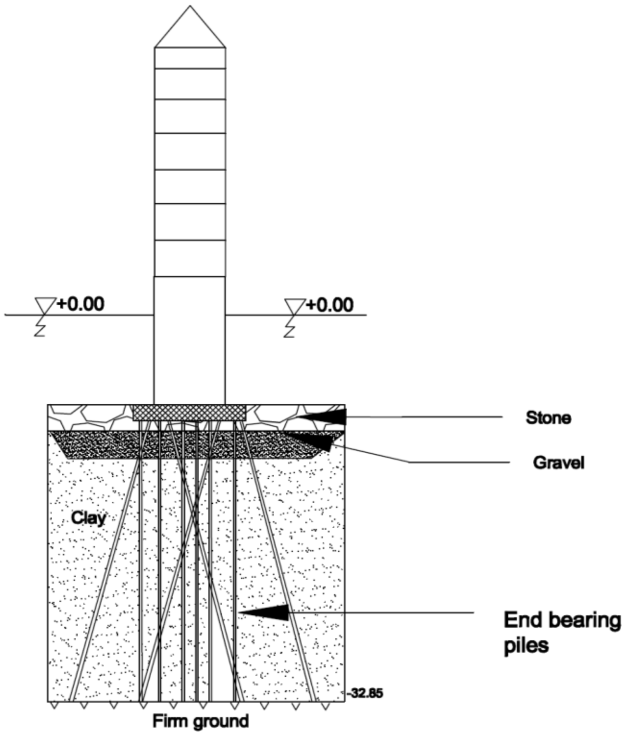

Figure 2.1 Section A-A

As shown in Figure 2.1, below the pile cap the ground is filled with gravel down to a depth of –12 m (the depth is measured from the water level) and stone is filled up to a depth of –8.85 m the top of the pile cap is located at –7.5 m.The clay extends to a depth of –33 m, Table 2.1 shows different parameters of the materials used in the foundation and the fill.

Table 2.1 Material properties of the soil

Material	Unit weight over water table [kN/m^3]	Unit weight under water table [kN/m^3]	Friction angle [^{0}]	Undrained Shear Strength [kPa]
Stone	18	11	35	-
Gravel	18	11	35	-
Clay	16	6	-	Varied [1]

2.2.2 Embankment

The embankment was built in 1998, to access the Eastern part of the tower by foot. The embankment is made of stone with properties as shown in Table 2.1, the upper part of the embankment is filled with Macadam (washed stone product 32 –64mm) underlain by less coarse gravel material(Forsberg et al, 2002).The dimension of the embankment is variable across its length. It is deep close to the tower and become shallower far away from the tower. The length of the embankment is around 57m.

[1] The variation of undrained shear strength is shown in equation 5.4.

3 The Eastern Tower

Both the eastern and western tower are constructed in the same way except to some minor differences like the depth of foundation and the availability of a gate on the western tower, to allow boats to pass. The stability of the western tower has been studied using a computation programme called SLIDE and it is found that the foundation is stable against slide (Forsberg et al, 2002). Moreover, since there is no earth pressure applied in this tower, the tower is assumed to be stable due to lateral force, therefore the stability study of the western tower is not included.

3.1 Timber Pile foundation

The tower is supported on a pile foundation, which is composed of two different types of piles, vertical and battered pile. There are 66 piles in total, 12 of which are battered with a slope of 1:4 and the rest are vertical piles. The average depth in which the piles are fixed is -33 meter measured from the water level. The head of the pile is located at-7.5 m and it is fixed in the pile cap, which is made out of reinforced concrete. The tips of the piles are rested on a firm stratum consequently; the piles are designed as end bearing piles for the vertical load. The arrangement of the pile group is shown in Figure 3.1.

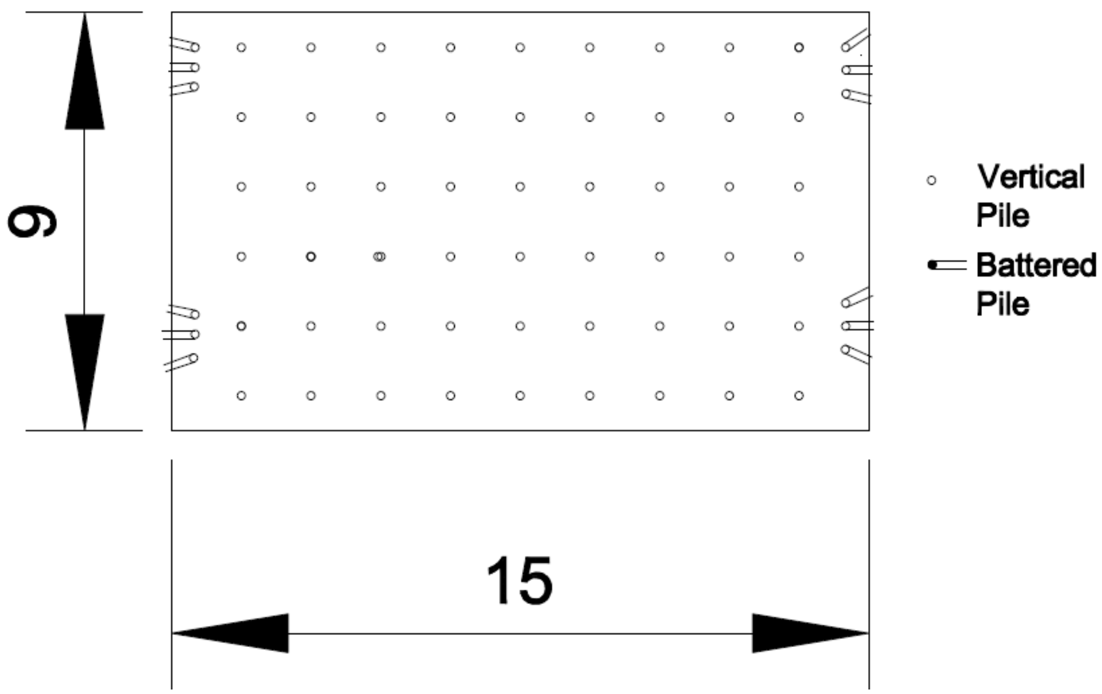

Figure 3.1 The plan view of pile cap showing the arrangement of piles

The pile foundation is made of wood, which is a typical foundation material at the time the foundation was constructed. It has been close to a century since the tower is built; therefore it is very important to look into different conditions in which the pile has been subjected, which potentially affect its load carrying capacity.

When wood piles are considered decaying is by far the most important factor, which leads to the deterioration of the piles. In order for a wood pile to decay air, free moisture and moderate temperature should be available (Keith F. Faherty and Thomas G. Williamson, 1997). Timber piles decay due to living microbes and they need two ingredients to thrive namely, oxygen and moisture. For timber piles to decay, both oxygen and moisture must be present (Ibid). Below the groundwater level, there is ample moisture but very little oxygen.

Timber piles submerged in groundwater will not decay. Oxygen is needed for the fungi (wood decaying microbes) to grow and below groundwater level, there is no significant amount of air in the soil. For this reason, very little decay occurs below the groundwater level (Ibid). Since the piles in this case are always located underwater they are considered to be free of decaying.

Timber piles usually have a varying cross sectional area, which results in different sectional properties and also the end bearing capacity of the pile is highly dependent on the cross sectional area of the tip of the pile. In this pile group all piles are assumed to have the same diameter, which equals 7 inches (178 mm) at the tip.

The type of timber used in the piles is softwood species which is common to the area. The strength properties of softwood is given in Eurocode 5 of prEN338:2002 and it is also presented in the appendix III , according to this code the class for the strength properties varies from C14 to C50, which means C14 is the weakest whereas C50 is the strongest. The timber used in this area conform to class C40 but a conservative assumption could be C35 and the strength properties of the piles taking class C35 is presented in Table 3.1.

Table 3.1 Strength properties of Timber piles, C35 according to prEN338:2002

Properties	Characteristic values
Bending	35 MPa
Tension parallel	21 MPa
Compression Parallel	25 MPa
Shear	3.4 MPa
Mean modulus of elasticity parallel	13 Gpa
5% modulus of elasticity parallel[1]	8.7 GPa
Mean Density	480 kg/m^3

[1] 5% accounts for the buckling of the pile under vertical load.

3.2 Pile Cap

Pile cap is necessary to distribute the load from the super structure to the piles. As shown in Figure 3.1 the pile cap measures 15 in length and 9 meter in width and the thickness is 1.3 meter. The pile cap is made out of reinforced concrete and its unit weight is equal to 25 kN/m^3.

3.3 Effect of Scour

Scour is the erosive action of flowing water, which is resulted when the shear stress generated from the flowing water exceeds the threshold value of the soil erosion resistance (Li .et al, 2009). Scour can be divided into two Local scour and general scour, the former refers to the erosion of material around the pile whereas the later is due to the erosion of relatively large area of the river bed (Ibid). The sum of local scour and global scour gives the total scour around the pile.

The presence of obstruction in the water bodies affects the flow pattern and ultimately increases the scour. Moreover, according to (Sharma, 1973), the size of the bed material and the flow depth play an important role.

Most researchers who have studied scour focused on solid piers and less attention were given for the effect of pile group, which are capped under water. In their study, (Salim and Jones, 1996) have determined different factors that could affect the scour depth. The factors they considered include spacing between piles, skew angle of flow, and pile cap location in reference to undisturbed stream bed.

In their experimental investigation, (Sumer et al, 2005) come up with, an empirical formula relating the scour depth with the size of the pile and the configuration of the pile group. Figure 3.2 shows the different type of pile group configuration used in the experiment and the result obtained are presented in table 3.2.

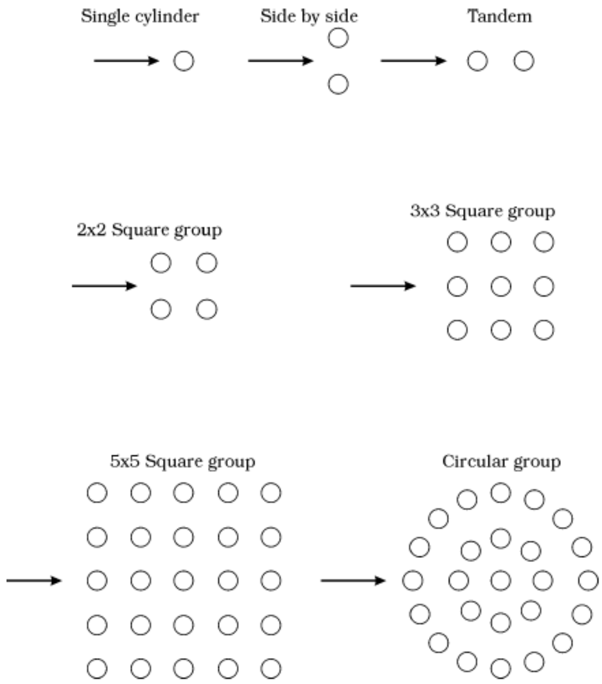

Figure 3.2 Pile group Configuration used in the experiment (Sumer et al, 2005)

Table 3.1 Equilibrium scour depth for the tested pile group

Pile group	Maximum *total* scour depth, S_T/D	Maximum *global* scour depth, S_G/D	Maximum *local* scour depth, S_{local}/D
Single pile	1.1	-	1.1
Side by side	1.5	0.78	0.70
2x2 square group	1.2	0.37	0.85
3x3 square group	1.8	0.92	0.90
5x5 square group	2.05	1.2	0.85
Circular group	2.6	1.5	1.1

The experiment is conducted for gap (Spacing between piles) to pile diameter ratio of 4, as can be seen in the above table the scour increases as the number of piles in the group increases. For 5x5 square pile group and for a pile diameter of 0.178 m the total scour will be 0.365 m.Since the number of piles in our pile group is more than this one a higher scour is expected, on the other hand since the pile spacing to pile diameter ratio is very large the effect of the scour will be less combining this two conditions a scour depth of 0.5 m is a good approximation.

4 ACTION FORCES ON THE TOWER

The pile foundation is loaded with both vertical (Self weight of the tower) and horizontal loads, which are resulted from wind pressure, water pressure and earth pressure. As previously mentioned the most important loads which destabilize the tower are the horizontal forces. The vertical force can cause some moment which depend on the eccentricity of the centre of gravity of the tower. Otherwise the foundation can be considered stable due to vertical forces.

4.1 Partial Factors for Action and Soil Strength parameters

Computation of action effects and soil strength parameters involve a lot of uncertainties, hence application of safety factors, to minimize the risk of failure is common. For Geotechnical structures, Eurocode 7, provide partial factor of safety for three different cases as shown in Table 4.1.

In order to assist the integration of Eurocode 7 with the other Eurocodes for structural material, three cases of partial factor of safety were introduced. In the ENV version of Eurocode 7 for geotechnical ultimate limit state, three cases, namely, Case A; Case B and Case C were adopted. The reason for these three cases is as follows (Trevor, 2006).

Case A considers uncertainties in the permanent and variable actions in situation where the strengths of the structure and the ground are insignificant in ensuring stability. It is relevant in situations where equilibrium depends primarily on the weight, with little contribution from the soil strength, and where hydraulic forces like buoyancy (uplift) are often the main loads.

Case B deals primarily with uncertainties in actions and hence the partial factors on actions in this case are generally greater than unity while the partial factors on ground parameters are equal to unity. Case B is usually critical in the structural design of elements such as foundations and retaining walls.

Case C deals primarily with uncertainties in ground parameters and hence the partial factors on the soil strength are greater than unity. In the case of piles and anchorages, however, the material factors are equal to unity and resistance factors greater than unity are used. Case C is usually critical in determining the sizes of elements in the ground, such as the size of foundations and retaining walls.

Table 4.1 Partial factors for cases A, B and C in ENV Eurocode[1]

Parameter	Symbol	Case A	Case B	Case C
Partial factors on actions or action effects(γ_F)				
Permanent unfavourable action	γ_G	1.0	1.35	1.0
Variable unfavourable action	γ_Q	1.50	1.5	1.3
Permanent favourable action	γ_G	0.95	1.0	1.0
Variable favourable action	γ_Q	0	0	0
Accidental action	γ_A	1.0	1.0	1.0
Partial factors for soil parameters (γ_M)				
Angle of shearing resistance (this factor is applied to $\tan\phi'$)	$\gamma_{\tan\phi'}$	1.1	1.0	1.25
Effective cohesion c'	$\gamma_{c'}$	1.3	1.0	1.6
Undrained shear strength c_u	γ_{cu}	1.2	1.0	1.4
Unconfined strength q_u	γ_{qu}	1.2	1.0	1.4
Presuremeter limit pressure, p_{lim}	γ_{plim}	1.4	1.0	1.4
CPT resistance	γ_{CPT}	1.4	1.0	1.4
Weight density of ground γ	γ_γ	1.0	1.0	1.0

As (Geoffrey, 1994) stated, geotechnical problems divided into two, stability problem and elasticity problem, which are now commonly called ultimate limit state and serviceability limit state problems, respectively. According to (Trevor, 2006) when designing using ENV of Eurocode 7 for ultimate limit state involving failure in the ground, it is important to carry out two separate calculations to check the design using two different partial safety factor applied in the action effect and soil parameters. This basically means, Case B and Case C will be used in the calculation, but in most cases Case C governs. When using serviceability limit state a partial factor of safety of unity will be used both in the action effects and the characteristic value of the soil parameter (Eurocode 7, Geoffrey, 1994, Trevor, 2006).

In line with the above argument, the calculation of the action effects, resisting forces and the subsequent analysis will be performed according to

Ultimate limit state using partial factor of safety for Case B and Case C
Serviceability limit state, with partial factor of safety of unity.

4.2 Wind Load

The climate change that is occurring in recent time has a direct effect on wind speed. In some part of the world like Iowa it has been recorded that the wind speed has continually reducing causing problem on wind turbines productivity (Science Daily June 26, 2009). On the other hand climate change has resulted in an increase of wind speed by 8% in Northern Europe (Martin L.Parry, 2007).

[1] In the EN version the design cases are somewhat revised.

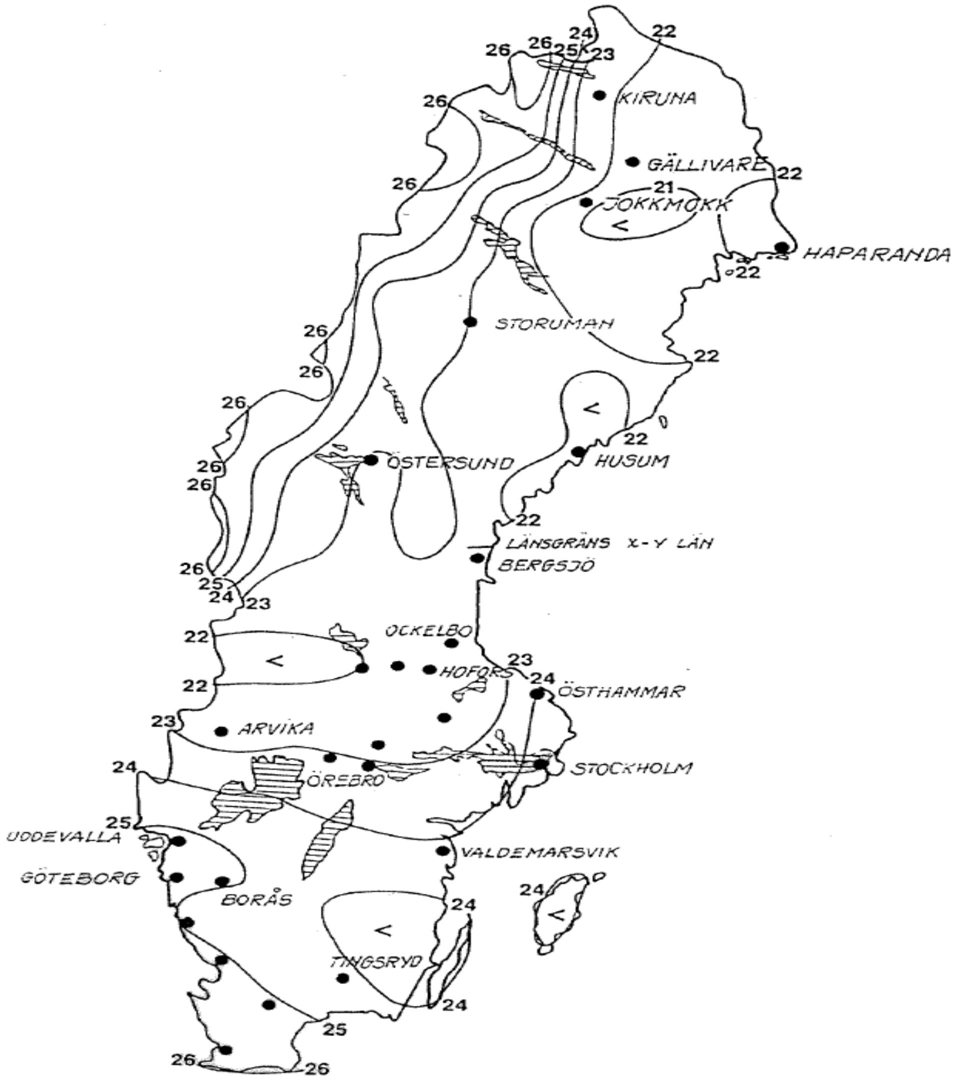

Figure 4.1 Reference wind speed [m/s] in Sweden

Wind load can be applied in any direction to the tower and all sorts of wind pressure should be investigated, particularly the one blowing in the west direction is very important since it can be combined with the earth pressure applied due to the embankment.

According to Eurocode, EN 1991-1-4 the wind actions are calculated from basic values of wind velocity or the velocity pressure. In accordance with EN 1990 4.1.2 (7) P basic values in the prediction of design wind velocity has a return period (mean recurrence interval) of 50 year. A 50 year return period wind speed has a probability of occurrence of 0.02 in any one year.

According to EN 1991-1-4 the wind forces acting on a whole structure or a structural component can be determined by either calculating forces using force coefficient or by calculating forces using surface pressure.

Wind pressure for the external and internal surfaces can be given as

$$W_e = q_p(Z_e) * C_{pe} \quad \text{and} \quad W_i = q_p(Z_i) * C_{pi} \qquad (4.1)$$

Where C_{pe} and C_{pi} are the pressure coefficient for the external and internal pressure respectively and q_p is peak velocity pressure.

Internal pressure develops due to opening on a building. Even if internal pressure is greater than 0, the net internal pressure of the whole structure is normally 0. Hence, the net pressure on the structure can be considered to be equal to the sum of external pressures.

The peak and basic velocity pressures are given in equation (4.2)

$$q_p(Z) = C_e(Z) * q_b \quad \text{and} \quad q_b = 1/2 \rho V_b^2 \qquad (4.2)$$

Where: $C_e(Z)$ is exposure factor shown in Fig 4.2, for different terrain category, at different height above the ground.

The air density is ρ =1.25kg/m3 and for Gothenburg from Fig 4.1 the basic wind velocity is V_b =25m/s. When we account the increase in wind speed due to climate change as given by (Martin L.Parry, 2007) we will get

$$V_{bnew} = 25 + 25 \cdot 0.08 = 27 \, \text{m/s}$$

Where: V_{bnew} is the basic wind speed after climate change.

Substituting these values in to equation (4.2) the basic velocity pressure becomes

$\Rightarrow$ q_b = 456kg/m.s^2 = 0.456kN/m^2

To find out the exposure coefficient the terrain category must be determined. The studied area has low vegetation near the facility and fewer obstacles (trees, buildings) which are also placed at least 20 obstacle heights away. Hence, according to PrEN 1991-1-4:2004, annex A, the place lays in category II. Having determined the terrain category, Figure 4.2 can be used to get the exposure coefficient at different height above the ground, Z.

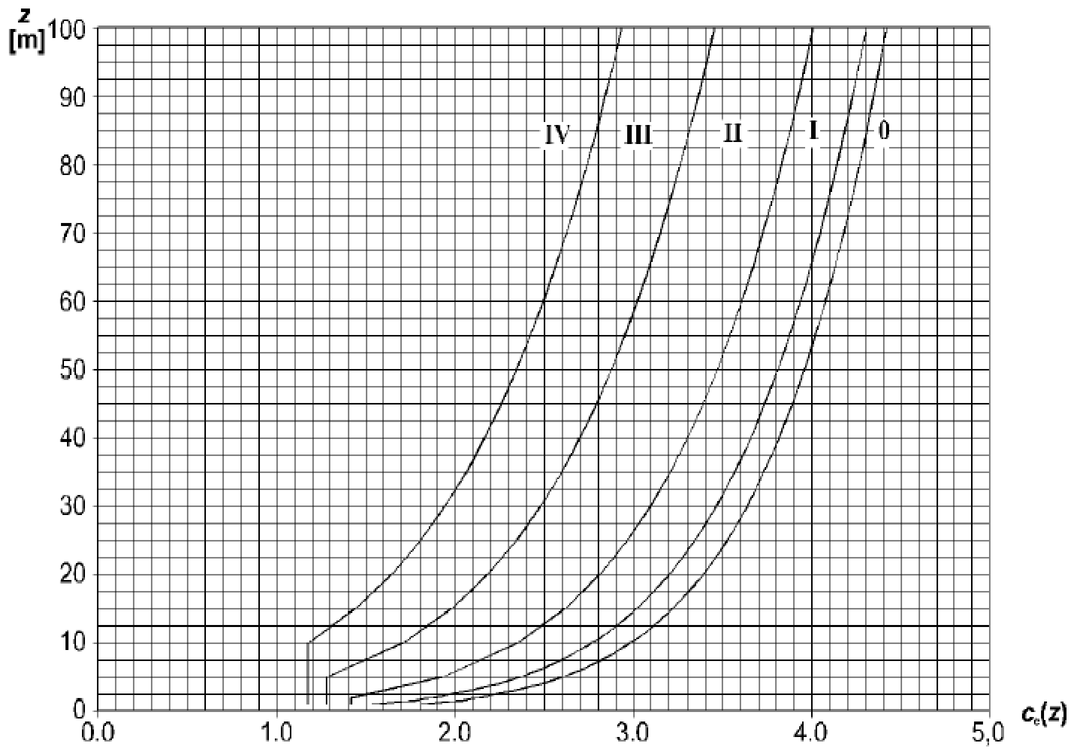

Figure 4.2 Exposure coefficient $C_e(Z)$ for C_o =1 and C_r =1

The peak velocity pressure, $q_p(Z)$, which is used to calculate the wind pressure can be calculated using Figure 4. 2 and equation (4.2), to do that the reference height, Z_e must be calculated first. According to PrEN 1991-1-4:2004 for structures with height greater than two times the width, b, (in the wind direction) can be considered to be multiple parts with lower part extending upward from ground by height equal to b and the upper part extending down ward from the top of the structure by length equals b and in between them middle part divided in to horizontal strips with height equals h_{strip} Figure 4.3 shows reference height and the corresponding velocity pressure.

Calculation of $q_p(Z)$ and W_e

H=25.45m, b= 5.66m h_{strip} =2m

Lower part

Z_e = 5.66m, $C_e(Z)$= 2

$\Rightarrow$ q_{pl} (5.66)= 2*0.456KN/m^2=0.912kN/m^2

Upper part

$Z_e = H$ = 25.45m, $C_e(Z)$= 3

$\Rightarrow$ q_{pu} (25.45)= 3*0.456KN/m^2=1.368kN/m^2

Middle Part

Dividing the middle part in to a strip of height 2.02m and seven strips the peak velocity pressure q_i can be calculated as above hence,

$q_{p1}(7.68)$= 2.18*0.456KN/m^2=0.994kN/m^2

$q_{p2}(9.7)$= 2.45*0.456KN/m^2=1.117kN/m^2

$q_{p3}(11.72)$= 2.5*0.456KN/m^2=1.140kN/m^2

$q_{p4}(13.74)$= 2.55*0.456KN/m^2=1.163kN/m^2

$q_{p5}(15.76)$= 2.65*0.456KN/m^2=1.208kN/m^2

$q_{p6}(17.78)$= 2.7*0.456KN/m^2=1.231kN/m^2

$q_{p7}(19.8)$= 2.8*0.456KN/m^2=1.277kN/m^2

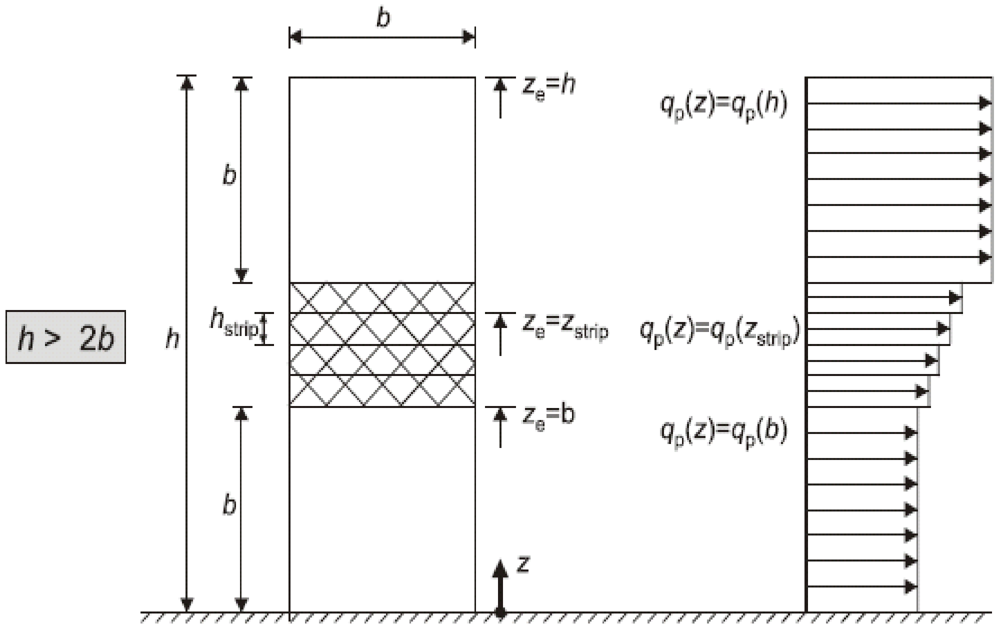

Figure 4.3 Reference heights, Z_e *depending on h and b and corresponding velocity pressure profile*

The final step in calculating the wind pressure is to determine the pressure coefficient and multiplying it with the peak velocity pressure. Figure 4.4 and Table 4.2 shows the external pressure coefficient for different zones.

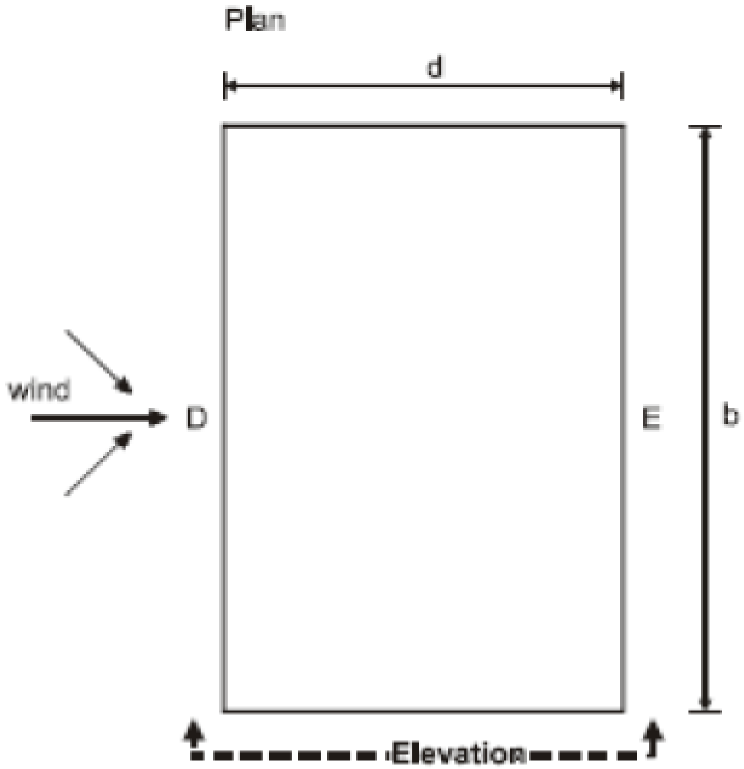

b: Crosswind dimension

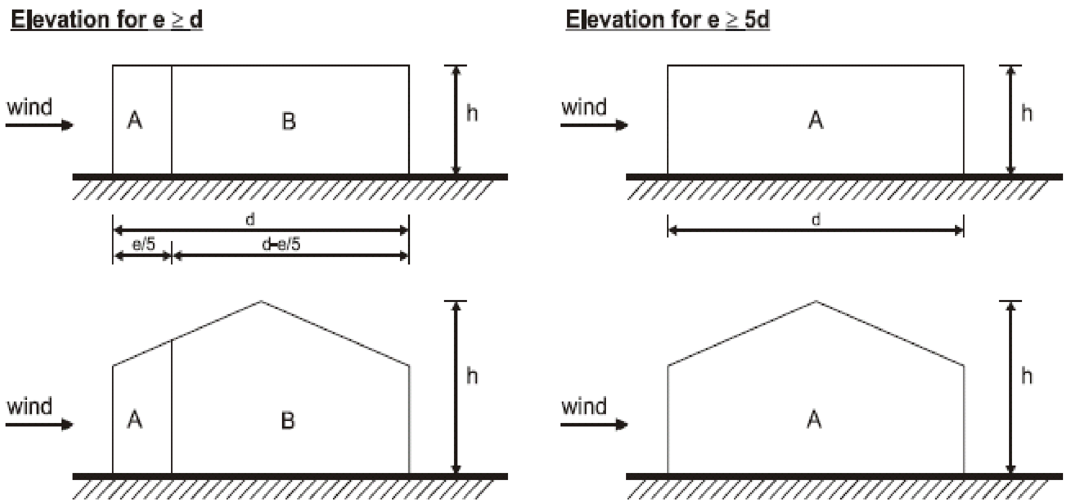

Figure 4.4 External pressure coefficients

e=b or 2h whichever is smaller

Table 4.2 Recommended values of external pressure coefficient for vertical walls of rectangular plan buildings

Zone	A		B		C		D		E	
h/d	$c_{pe,10}$	$c_{pe,1}$	$c_{pe,10}$	$c_{pe,1}$	$c_{pe,10}$	$c_{pe,1}$	$c_{pe,10}$	$c_{pe,1}$	$c_{pe,10}$	$c_{pe,1}$
5	-1,2	-1,4	-0,8	-1,1	-0,5		+0,8	+1,0	-0,7	
1	-1,2	-1,4	-0,8	-1,1	-0,5		+0,8	+1,0	-0,5	
≤ 0,25	-1,2	-1,4	-0,8	-1,1	-0,5		+0,7	+1,0	-0,3	

For intermediate values of h/d, linear interpolation may be applied.

As can be shown in Table 4.2 except zone D all zones are under suction (negative pressure) more over the pressure direction is predefined as the stability of the tower is affected by the wind pressure and the earth pressure due to the embankment. Therefore, Zone D and Zone E are the most important zones regarding stability of the tower.

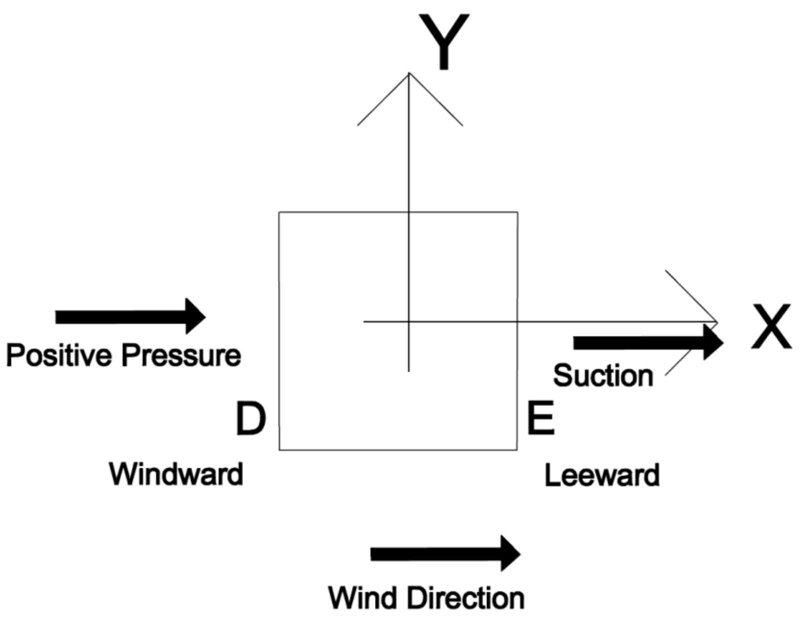

Figure 4.5 Distribution of wind load on the structure

The Total wind pressure on the structure is the sum of positive pressure on the windward direction (Zone D) and the suction on the leeward direction (Zone E). As can be seen from Table 4.2 the external pressure coefficient for Zone D is equal to 0.8 where as in Zone E interpolation between 0.5 and 0.7 will be done for various values of h/d. Hence, using equation (4.1) the wind pressure can be calculated as:

$W_{el} = (0.8 + 0.5) \cdot 0.91\,\text{kN/m}^2 = 1.19\text{kN/m}^2$

$W_{eu} = (0.8 + 0.67) \cdot 1.37\,\text{kN/m}^2 = 2.01\text{kN/m}^2$

$W_{e1} = (0.8 + 0.52) \cdot 0.99\,\text{kN/m}^2 = 1.31\text{kN/m}^2$

$W_{e2} = (0.8 + 0.54) \cdot 1.12\,\text{kN/m}^2 = 1.50\text{kN/m}^2$

$W_{e3} = (0.8 + 0.55) \cdot 1.14\,\text{kN/m}^2 = 1.54\text{kN/m}^2$

$W_{e4} = (0.8 + 0.57) \cdot 1.16\,\text{kN/m}^2 = 1.59\text{kN/m}^2$

$W_{e5} = (0.8 + 0.59) \cdot 1.21\,\text{kN/m}^2 = 1.68\text{kN/m}^2$

$W_{e6} = (0.8 + 0.61) \cdot 1.23\,\text{kN/m}^2 = 1.73\text{kN/m}^2$

$W_{e7} = (0.8 + 0.62) \cdot 1.28\,\text{kN/m}^2 = 1.82\text{kN/m}^2$

The wind force (characteristic value) in kN is calculated by multiplying, the wind intensity acting on the tower at certain elevation from the ground, by the corresponding projected area of the tower.

$$F_{wk} = W_e \cdot A_i \qquad (4.3)$$

Where, W_e is the wind pressure acting at a distance X_i from the ground and A_i is the corresponding projected area perpendicular to the wind direction

$F_{wl} = 1.19 \cdot (5.66 \cdot 5.66) = 38.12\,\text{kN}$

$F_{wu} = 2.01 \cdot (5.66 \cdot 5.66) = 64.39\,\text{kN}$

$F_{w1} = 1.31 \cdot (5.66 \cdot 2.02) = 14.98\,\text{kN}$

$F_{w2} = 1.5 \cdot (5.66 \cdot 2.02) = 17.15\,\text{kN}$

$F_{w3} = 1.54 \cdot (5.66 \cdot 2.02) = 17.61\,\text{kN}$

$F_{w4} = 1.59 \cdot (5.66 \cdot 2.02) = 18.18\,\text{kN}$

$F_{w5} = 1.68 \cdot (5.66 \cdot 2.02) = 19.21\,\text{kN}$

$F_{w6} = 1.73 \cdot (5.66 \cdot 2.02) = 19.78\,\text{kN}$

$F_{w7} = 1.82 \cdot (5.66 \cdot 2.02) = 20.81\,\text{kN}$

The design value of the wind force for Case B and Case C can be calculated using the following equation.

$$F_{wdB} = \gamma_{QB} \cdot F_{wk} \qquad (4.4)$$

$$F_{wdC} = \gamma_{QC} \cdot F_{wk} \qquad (4.5)$$

As give in Table 4.1 the value of $\gamma_{QB} = 1.5$ and $\gamma_{QC} = 1.3$, hence

Design wind load for Case B	Design Wind Load for Case C
$F_{wldB} = 1.5 \cdot 38.12 = 57.18\,\text{kN}$	$F_{wldC} = 1.3 \cdot 38.12 = 49.56\,\text{kN}$
$F_{wudB} = 1.5 \cdot 64.39 = 96.59\,\text{kN}$	$F_{wudC} = 1.3 \cdot 64.39 = 83.71\,\text{kN}$
$F_{w1dB} = 1.5 \cdot 14.98 = 22.47\,\text{kN}$	$F_{w1dC} = 1.3 \cdot 14.98 = 19.47\,\text{kN}$
$F_{w2dB} = 1.5 \cdot 17.15 = 25.73\,\text{kN}$	$F_{w2dC} = 1.3 \cdot 17.15 = 22.30\,\text{kN}$
$F_{w3dB} = 1.5 \cdot 17.61 = 26.42\,\text{kN}$	$F_{w3dC} = 1.3 \cdot 17.61 = 22.89\,\text{kN}$
$F_{w4dB} = 1.5 \cdot 18.18 = 27.27\,\text{kN}$	$F_{w4dC} = 1.3 \cdot 18.18 = 23.63\,\text{kN}$
$F_{w5dB} = 1.5 \cdot 19.21 = 28.82\,\text{kN}$	$F_{w5dC} = 1.3 \cdot 19.21 = 24.97\,\text{kN}$
$F_{w6dB} = 1.5 \cdot 19.78 = 29.67\,\text{kN}$	$F_{w6dC} = 1.3 \cdot 19.78 = 25.71\,\text{kN}$
$F_{w7dB} = 1.5 \cdot 20.81 = 31.22\,\text{kN}$	$F_{w7dC} = 1.3 \cdot 20.81 = 27.05\,\text{kN}$

4.3 Lateral Earth Pressure

Lateral earth pressure is a significant design element in a number of foundation engineering problem, retaining structures require a quantitative estimate of the lateral pressure on a structural member for either a design or stability analysis (Bowles, 1997). Basically, there are three different types of lateral earth pressure as shown on the Mohr rupture envelop Figure 4.6, they can be stated as pressure at rest, active earth pressure and passive earth pressure.

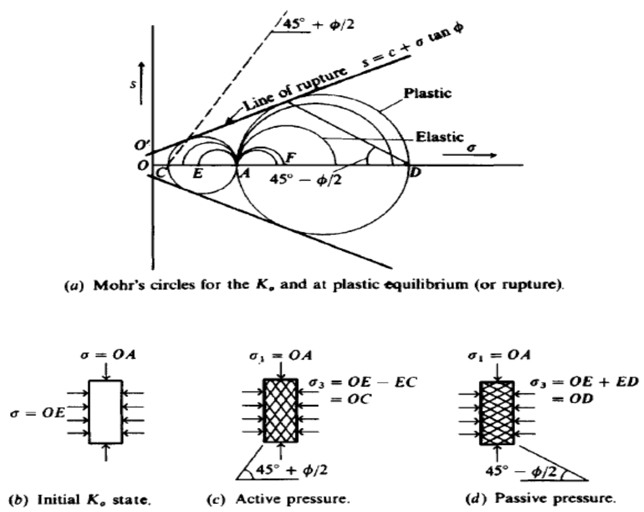

Figure 4.6 Illustration of the concept of elastic and plastic equilibrium. The stresses in (b),(c) and (d) such as OA,OE,EC are identified on the Mohr's circles of (a) (Bowels 1997)

Even though earth pressure develops as the soil start to move, the stresses are indeterminate until the soil is on the verge of failure as shown on the Mohr's rapture envelop and depending on the mode of displacement of the wall the stress at failure could be either active or passive (Ibid).

The lateral earth pressure applied to the tower due to the embankment is active earth pressure as the tower is moving away from the embankment but if there is no sufficient lateral displacement of the wall, the lateral pressure will not reach plastic equilibrium, and hence the active pressure will not be mobilized. The wall must displace or rotate by a minimum amount, which is enough to produce active earth pressure as shown by a line OC in Figure 4.6; these minimum displacements has been investigated in the past, and are presented in Table 4.3.

Table 4.3 Guide line values of rotation/displacement sufficient to develop active earth pressure (Bowels 1997)

Soil and condition	Amount of translation, $\delta_{h,a}$
Cohesionless, dense	0.001 to 0.002H
Cohesionless, loose	0.002 to 0.004H
Cohesive, firm	0.01 to 0.02H
Cohesive, soft	0.02 to 0.05H

Assuming the amount of lateral displacement, $\delta_{h,a}$ as presented in the above table is satisfied in our case, earth pressure theories can be used to calculate the amount of active lateral earth pressure.

There are two commonly used theories to calculate lateral earth pressure

Rankine Earth pressure theory

Coulomb Earth Pressure Theory

The Rankine theory assumes

- There is no adhesion or friction between the wall and soil

- Lateral pressure is limited to vertical walls

- Failure in the back fill occurs as a sliding wedge over an assumed failure plain defined by ϕ (friction angle of the backfill).

-Lateral pressure varies linearly with depth and the resultant pressure is located one third of the height (H) above the base of the wall.

- The resultant force is parallel to the back fill surface

The coulomb theory is similar to Rankine except

- It takes into account the friction between the wall and the back fill.

- The lateral pressure is not limited to a vertical wall

- The resultant force is not necessarily parallel to the back fill because of the soil wall friction.

Since the lateral pressure in this problem is applied on vertical wall and neglecting the friction between the wall and the soil as the area is relatively small, Rankine earth pressure theory can be used to calculate the lateral pressure.

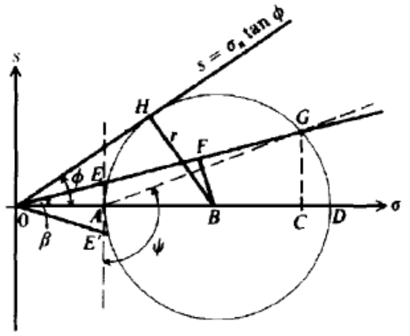

Figure 4.7 Mohr's circle to derive the Rankine earth pressure equation

Figure 4.7 can be used to derive the active earth pressure coefficient, K_a. K_a, can be given as the ratio between OE and OG as shown in the above Figure. After using trigonometric relation and simplifying we can get the value K_a to be as shown in equation (4.7).

$$K_a = \cos\beta \frac{\cos\beta - \sqrt{\cos^2\beta - \cos^2\phi}}{\cos\beta + \sqrt{\cos^2\beta - \cos^2\phi}} \qquad (4.7)$$

In the above equation β is the inclination of the backfill against the horizontal and ϕ is the angle of internal friction of the back fill. Since the inclination of the backfill is zero and by using trigonometric identities the above equation can be reduced to a more simple equation, which is given by equation (4.8).

$$K_a = \frac{(1-\sin(\phi))}{(1+\sin(\phi))} \qquad (4.8)$$

The friction angle as given in Table 2.1 is equal to 35^o before calculating the active earth pressure coefficient; we have to apply the partial factor of safety on the soil parameter. As shown in Table 4.1 the partial factor of safety for the angle of internal friction is applied on $\tan\phi$.The partial factor for Case B and Case C are given below.

For Case B: $\gamma_{\tan\phi B} = 1$ and for Case C: $\gamma_{\tan\phi C} = 1.25$ hence

$$\phi_d = \arctan(\frac{\tan\phi}{\gamma_{\tan\phi}}) \tag{4.9}$$

By substituting the partial factors on equation (4.9) we get the design value of angle of internal friction as

$\phi_{dB} = 35^0$ and $\phi_{dC} = 29^0$ finally substituting these values in to equation (4.8) gives the active earth pressure coefficients.

$\Rightarrow$ $K_{adB} =$ 0.27 and $K_{adC} =$ 0.35

The value of lateral earth pressure in 2D is given by

$$P_a = \tfrac{1}{2} K_a \gamma' H^2 \quad \text{And} \quad \gamma' = \gamma - \gamma_w \tag{4.10}$$

Where γ' is the effective or submerged unit weight of the soil which is equal to the total unit weight, γ, of the backfill minus the unit weight of water.

$\gamma' = 11$ kN/m^3 from Table 2.1 and H=7.5 m where H is the height of the embankment substituting these values in to equation (4.10)

$P_{aB} =$ 83.84 kN/m, and $P_{aC} =$ 108.28 kN/m these forces are located 2.5 m above the base of the embankment for both Cases.

4.3.1 Correction for wall size

The earth pressure using the classical formulas of rankine or columbs can be used for walls with infinite length with the assumption of 2D earth pressure distribution, but when the wall is short, 3D earth pressures will be mobilized. According to DIN (German institute for Standardization) since the wall be deflecting more the active earth pressure mobilized will be smaller. In order to account this effect the length, where the earth pressure acts should be corrected to a new length L_{new} which is shorter than L.

For a single layer soil the new characteristic earth pressure, $E_{new,k}$ is given as

$$E_{new,k} = P_a \cdot L_{new} \tag{4.11}$$

Where, $E_{new,k}$ is earth pressure in kN.

$$L_{new} = L \cdot \left\{ 1 - \frac{2}{\Pi} \cdot \left[\left(1 + \frac{1}{A^{*2}} \right) \cdot \arctan A^* - \frac{1}{A^*} \right] \right\} \tag{4.12}$$

Where, $A^* = \dfrac{\phi \cdot H}{2 \cdot L}$ and ϕ is given as radian

Hence, $A^{*} = \frac{0.611 \cdot 7.5}{2 \cdot 5.66} = 0.405$

$$\Rightarrow L_{new} = 5.66 \cdot \left\{1 - \frac{2}{\Pi} \cdot \left[\left(1 + \frac{1}{0.405^2}\right) \cdot \arctan 0.405 - \frac{1}{0.405}\right]\right\}$$

$$L_{new} = 4.71\text{m}$$

Hence, the final corrected earth pressure E_{new} in kN with the assumption of 3D active earth pressure distribution will be

$$E_{new,\,kB} = 4.71 \cdot 83.84 = 395kN \text{ and } E_{new,\,kC} = 4.71 \cdot 108.28 = 510kN$$

The above calculated earth pressure is a characteristic value (since the partial factor of safety for action effect is not involved yet) hence; we need to calculate a design value which take into account the action effect as well. As given in Table 2.1the partial factor of safety for permanent action effect for Case B and Case C is given below.

$$\gamma_{GB} = 1.35 \quad \text{And} \quad \gamma_{GC} = 1.0$$

The design value of the Earth pressure is given by the

$$E_{new,dB} = \gamma_{GB} \cdot E_{new,kB} \tag{4.13}$$

$$E_{new,dC} = \gamma_{GC} \cdot E_{new,kC} \tag{4.14}$$

$$\Rightarrow E_{new,dB} = 1.35 \cdot 395 = 533kN$$

And $E_{new,dC} = 1.0 \cdot 510 = 510kN$

The load from the embankment calculated above is acted in the x- direction and added to the wind load, whereas the load from the water given in section 4.4 is in the y-direction.

4.4 Water Pressure

The water pressure applied on the tower in all direction is equal when the screen is open, however, when the screen is closed, there will be a water level difference between the upstream and downstream, which can reach a maximum level of 20 cm (Forsberg et al, 2002). This causes a pressure along the length of the screen, which finally transfers to the two supporting structures as shown in figure 1.2, which hold the screen. The pressure applied on the screen wall is assumed to be hydrostatic because the screen closes very slowly and the effect of dynamic pressure is negligible. Figure 4.7 shows the pressure distribution on the screen wall.

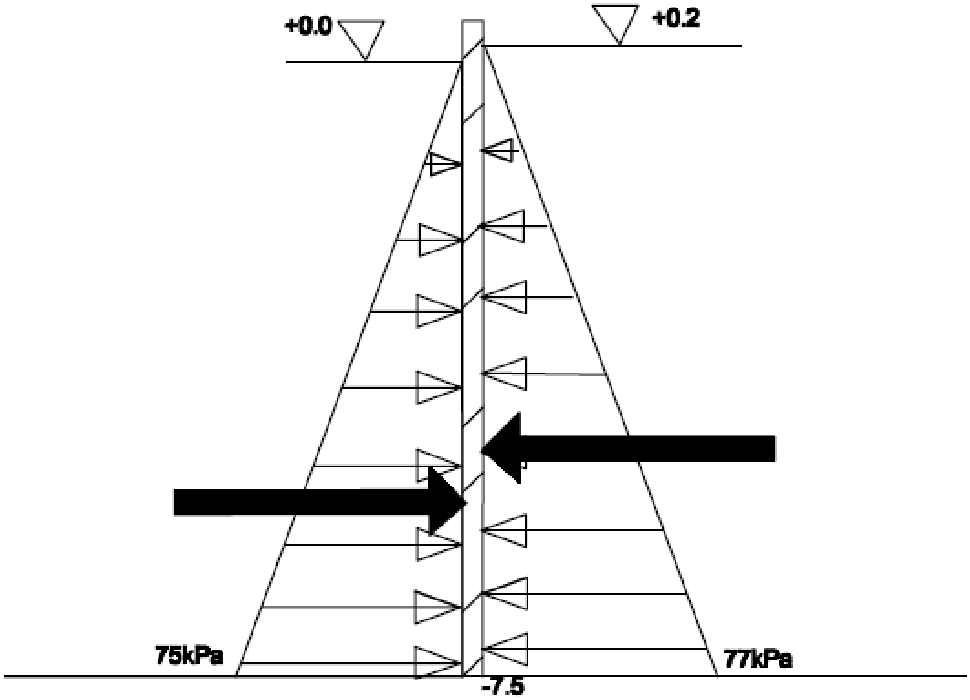

Figure 4.7 Water Pressure distribution on the screen when the screen is fully closed

As shown in the above figure, water pressure is applied on both sides since there is a water level difference, there will be a net pressure which is given as

$$P_{w,net} = P_{w,upstream} - P_{w,downstream} = 1/2 \cdot \gamma_w \cdot h_2 \cdot \Delta h + 1/2 \cdot \gamma_w \cdot h_1 \cdot \Delta h \quad (4.15)$$

Where:

$P_{w,upstream}$: Water pressure from the upstream

$P_{w,downstream}$: Water pressure from the downstream

γ_w : Unit weight of water

h_2 And h_1 : water level from the upstream and downstream side respectively

Δh : Water level difference

Substituting the values of the known variables into equation (4.15) one can get

$$P_{w,net} = 1/2 \cdot 10 \cdot 7.7 \cdot 0.2 + 1/2 \cdot 10 \cdot 7.5 \cdot 0.2 = 15.2 kN/m$$

To calculate the horizontal force applied on the wall, the net pressure will be multiplied by the length of the screen wall, l_{screen}. It is assumed that half of this force is transferred to the tower in question. Hence, the horizontal force (in the y- direction) applied on the tower is given by:

$$F_{water,k} = 1/2 \cdot P_{w,net} \cdot l_{screen} \tag{4.16}$$

Where:

l_{screen}: Length of screen which is equal to 43m

$$F_{water,k} = 1/2 \cdot 15.2 \cdot 43 = 326.8kN$$

And taking sum of moments about the toe of the wall it can be seen that the force is applied at 3.8 meter from the bottom of the wall. The design value of the action force using partial factor of safety is

$$F_{water,dB} = \gamma_{QB} \cdot F_{water,k} \tag{4.17}$$

$$F_{water,dC} = \gamma_{QC} \cdot F_{water,k} \tag{4.18}$$

Where:

$\gamma_{QB} = 1.5$ And $\gamma_{QC} = 1.3$

$\Rightarrow F_{water,dB} = 1.5 \cdot 326.8 = 490kN$

And $F_{water,dC} = 1.3 \cdot 326.8 = 425kN$

The moment resulting from the water load is given as

$$M_{dx} = F_{water,d} \cdot 3.8 \tag{4.19}$$

$M_{dBx} = 490 \cdot 3.8 = 1862kNm$

$M_{dCx} = 425 \cdot 3.8 = 1615kNm$

4.5 Total Force and Bending Moment on the Pile cap

The total lateral force in the x direction, F_k or F_d for the characteristic or design value, respectively acting at the base of the tower (Pile cap) is, the sum of all wind forces and earth pressure, which are acting at different arm length (X_i) and the bending moment M_k or M_d, which results from the above forces is calculated by multiplying these forces by their corresponding arm length (X_i).

$$M_{ky} = \sum F_{wk} \cdot X_i + E_{new,k} \cdot 2.5 \quad \text{And} \quad F_k = \sum F_{wk} + E_{new,k} \tag{4.20}$$

$$M_{dy} = \sum F_{wd} \cdot X_i + E_{new,d} \cdot 2.5 \qquad \text{And} \qquad F_d = \sum F_{wd} + E_{new,d} \qquad (4.21)$$

Where, F_{wk} or F_{wd} is wind force acting on the tower at X_i from the base of the tower

X_i is arm length.

All the characteristic action forces and the associated design values are summarized in Table 4.3 and Table 4.4, respectively.

Table 4.3 Summary of characteristic action effects from wind and backfill material

Elevation measured from the pile cap(m)	Wind pressure(kN/m^2)	Action force due to wind and backfill (kN)	Moment at the pile cap (kNm)
13.16	0.730	38.12	501.66
32.95	1.094	64.39	2121.65
15.18	0.795	14.98	227.40
17.20	0.894	17.15	295.00
19.22	0.912	17.61	338.46
21.24	0.930	18.18	386.14
23.26	0.966	19.21	446.82
25.28	0.985	19.78	500.00
27.30	1.022	20.81	568.11
2.50		510	987.50
$\sum$		**625.00**	**6373.00**

Table 4.4 Summary of design action effects from wind and backfill material

Elevation measured from the pile cap (m)	Action force due to wind and backfill (kN), Case B	Moment at the pile cap (kNm), Case B	Action force due to wind and backfill (kN), Case C	Moment at the pile cap (kNm), Case C
13.16	57.18	752.49	49.56	652.21
32.95	96.59	3182.64	83.71	2758.24
15.18	22.47	341.09	19.47	295.55
17.20	25.73	442.56	22.30	383.56
19.22	26.42	507.79	22.89	439.95
21.24	27.27	579.21	23.63	501.90
23.26	28.82	670.35	24.97	580.80
25.28	29.67	750.06	25.71	649.95
27.30	31.22	879.61	27.05	738.47
2.50	533.00	1332.5	510	1275
$\sum$	**878.00**	**9438.00**	**809.00**	**8276.00**

4.6 Vertical Force Due to Self Weight

The tower is made out of different material with varying unit weight. The material includes steel for the main frame, wooden and insulation material for the wall and reinforced concrete in the coussine and pile cap. The weight of the mechanical system, which is responsible for the lowering and lifting up of the water barrier, is considered to be equal to the weight of the tank filled with water and the counter weight.

Weight due to steel frame, $W_{steel} = L_{steel} \cdot 30kg/m \cdot 9.81m/s^2$

Where:

L_{steel} is the total length of steel bar.

$L_{steel} = 5.66 \cdot 4 \cdot 7 + 3 \cdot 4 \cdot 7 + 3.04 \cdot 4 \cdot 7 + 6 \cdot 4 \cdot 6 = 471.6m$

Hence, $W_{steel} = 471.6 \cdot 30 \cdot 9.81 = 138.79KN$

Weight due to wooden wall, $W_{wood} = A_{wood} \cdot 35kg/m^2 \cdot 9.81m/s^2$

Where:

A_{wood} is the total area of the wall.

$A_{wood} = 5.66 \cdot 25.45 \cdot 4 = 576.19m^2$

Hence, $W_{wood} = 576.19 \cdot 35 \cdot 9.81 = 197.83KN$

Weight due to reinforced concrete, $W_{concrete} = (V_{cassoun} + V_{pilecap}) \cdot 25KN/m^3$

$V_{cassoun} = 14 \cdot 9 \cdot 0.2 \cdot 2 + 5.66 \cdot 9 \cdot 0.2 \cdot 4 = 91.15m^3$

$V_{pilecap} = 14 \cdot 9 \cdot 1.35 = 170.1m^3$

Hence, $W_{concrete} = (91.15 + 170.1) \cdot 25 = 6531.00KN$

Therefore, the total vertical force due to self weight of the tower is

$F_{vk} = 138.79 + 197.83 + 6531.25 = 6868.00KN$

$$F_{vdB} = \gamma_{GB} \cdot F_{vk} \tag{4.22}$$

$$F_{vdC} = \gamma_{GC} \cdot F_{vk} \tag{4.23}$$

$\Rightarrow F_{vdB} = 1.3 \cdot 6867.87 =$ **8928.00kN**

And $F_{vdC} = 1.0 \cdot 6867.87 =$ **6868.00kN**

Table 4.5 Summary of design load.

Type of Load	Total Load Case B (kN)	Total Load Case C (kN)	Direction
Wind Load	345	299	X axis
Dead Load	8928	6868	Z axis
Earth Pressure	533	510	X axis
Water Pressure	490	425	Y axis

5 STABILITY ANALYSIS

The stability analysis is performed using software called, Geosuite. The computer program consists of soil data generator (GENSOD), a pile data generator (PILGEN) and the program, which solves the combined pile-soil interaction (SPLICE).

Two different soil model were available the first one is API (developed by American petroleum Institute) and the other one is NTNU(developed by Norwegian University of Science and Technology) due to the proximity of the regions and the availability of more knowledge regarding the later model it is decided to use NTNU soil model.

The undrained or drained soil properties used in the NTNU soil model are described below.

5.1 Undrained shear strength

To get the undrained shear strength of the clay soil underneath the granular soil the average value of undrained shear strength measured near the facility were taken. There were a number of boreholes made at the site with varying depth some extends a few meter while others reach up to 24 m below the ground level. In this investigation three boreholes are chosen this is because they are located very close to the tower as compared to other boreholes and moreover they measure undrained shear strength as deep as 24m. Table 5.1 and Figure 5.1 show the variation of undrained shear strength with depth. The CPT tests for the three boreholes are shown in Appendix IV, V and VI.

Table 5.1 Variation of Undrained Shear Strength with Depth

	Undrained Shear Strength(KPa)			
Depth(m)	2550V45	2550V90	2550+290	Average
2	8	12	10	10.00
4	10	14	15	13.00
6	18	15	20	17.67
8	22	22	25	23.00
10	24	25	28	25.67
12	27	30	34	30.33
14	32	28	36	32.00
16	34	32	42	36.00
18	32	38	42	37.33
20	30	40	46	38.67

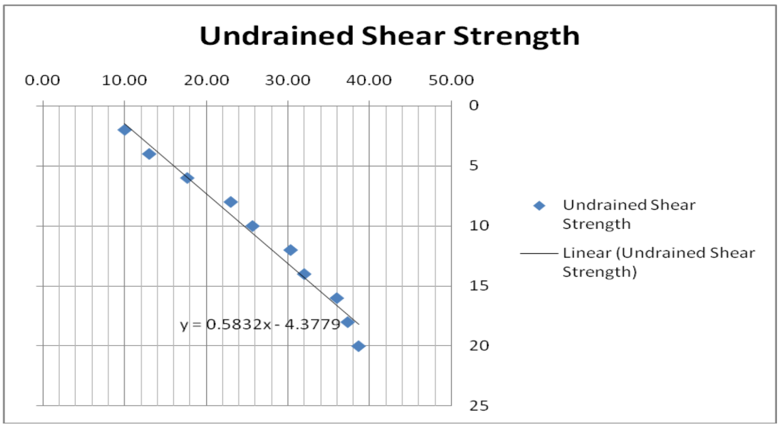

Figure 5.1 Average value of Undrained Shear Strength

By fitting a trend line on the graph for the average value of undrained shear strength, the equation for the undrained shear strength can be obtained and by rearranging it and using a proper notation the following equation can be derived.

$$C_{uk} = 1.71 \cdot Z + 7.51 \qquad (5.1)$$

The above equation gives the characteristic value of the undrained shear strength of the ground. As described before for the ultimate limit state analysis, the design value is required, hence using Table 2.1 for the partial factor of safety of the material parameters the following equation can easily be derived.

The value of the partial factors can be read from Table 2.1.

$$\gamma_{cuB} = 1.0 \quad \text{And} \quad \gamma_{cuC} = 1.4$$

$$C_{udB} = \frac{C_{uk}}{\gamma_{cuB}} = 1.71 \cdot Z + 7.51 \qquad (5.2)$$

$$C_{udC} = \frac{C_{uk}}{\gamma_{cuC}} = 1.22 \cdot Z + 5.36 \qquad (5.3)$$

In addition to the undrained shear strength, other soil parameters are used in the NTNU soil model. As shown in section 4.3, the angle of internal friction for Case B is 35^0 and for Case C 29^0. All the other parameters used in the model are summarized in table 5.2.

Table 5.2 Summary of soil parameters used in NTNU soil model

Parameters	Values in the first(granular soil) layer	Value in the second (clay soil) layer
Attraction	0 kN/m^2	10 kN/m^2
Pile soil roughness ratio	0.5	0.5
Horizontal stress ratio in soil at pile before loading	N.A	1
Vertical effective stress	58 kPa	178 kPa
Shear modulus number	1	1
Shear mobilization factor	N.A	0.7
Dilaitancy parameter	N.A	0.02
Horizontal stress in soil at pile when the soil fail	N.A	0.3
Mobilization exponent to the tangent shear modulus	N.A	2
Mobilization exponent to the modulus	1	N.A
Dilaitancy factor for over consolidated clay	N.A	1
Deformation reference stress	100 kPa	N.A
Janbu's stress exponent to the modulus function	1	N.A
Displacement factor	N.A	0.05

5.2 Nonlinear pile and p-y Model for soil

Among other factors, the behaviour of laterally loaded pile depends on the stiffness of the pile and the mobilization of soil resistance around the pile (Unified Facilities Criteria, Deep foundation, 2004).

In the p-y model, the soil around the pile is represented by a spring (Winkler's spring), which designate that the soil develops a resistance p when the pile deflect by a distance y. Figure 5.2a shows a uniform distribution of stress around the pile and Figure 5.2b shows stress distribution when the pile caused to deflect a distance y. The stress in the second case will decrease at the back side of the pile and increase on the front side, the integration of the stresses around the pile gives the quantity p which acts in the opposite direction to the deflection y.

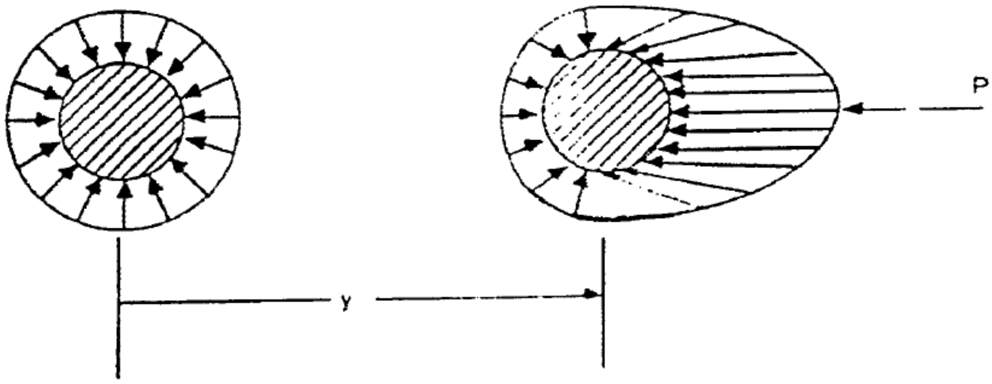

(a) Before Bending (b) After Bending

Figure 5.2 Distribution of stresses before and after lateral deflection (Unified Facilities Criteria, Deep foundation, 2004)

The p-y curve is basically accounts for the soil type and in our case we have two distinct p-y curves, the first shown in Figure 5.3, represent the lateral resistance of the soil in the ultimate limit state Case B and for the serviceability limit as well, this is due to the fact that the same partial factor of safety was used for the material property in both cases. The second type of p-y curve shown in Figure 5.4 represents the lateral resistance of the same soil whose material property is factored by partial factor of safety of 1.4. One thing should be noted here is the p-y curve varies along the length of the pile and the figure below show a representative point namely 0.96m from the ground and more p-y curves are presented on the appendix VII.

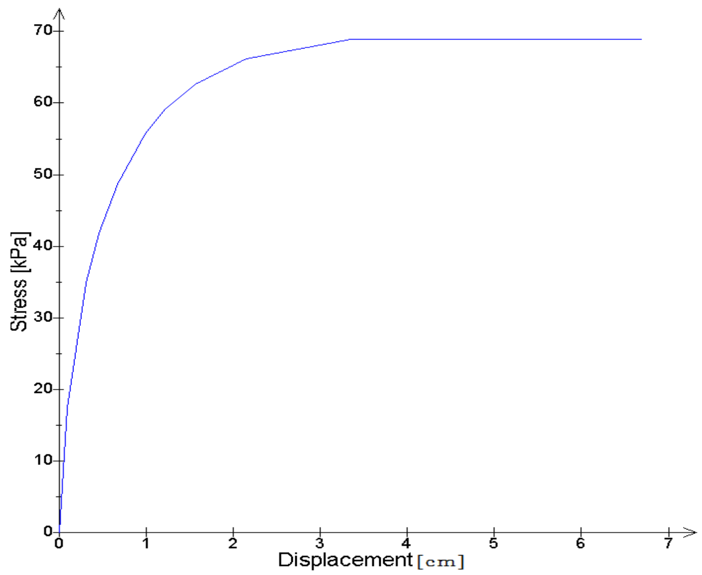

Figure 5.3 p-y curve for ultimate limit state Case B and for serviceability limit state at a depth of 0.96m.

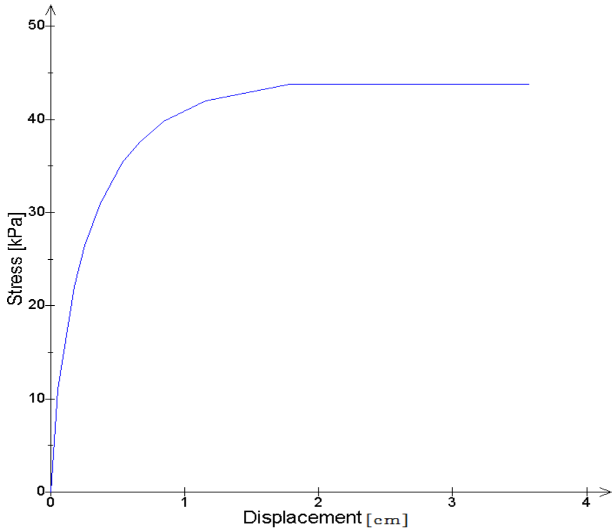

Figure 5.4 p-y curve for ultimate limit state Case C at a depth of 0.96m.

5.3 Structural Capacity of the Piles

Pile No. 58 and Pile NO.63 are the piles that need to be investigated as they are highly stressed. There are four cases considered in the calculation of the capacity of the pile. The first two cases consider maximum axial load on pile 58 and 63 when the screen open and closed. The other two cases is the maximum moment on pile 58 and 63. Calculation of maximum axial load is done by hand calculation because the program Geosuite pile group couldn't give results for a highly loaded pile (the iteration can't be converged).

The structural capacity of the pile is checked by calculating the combined effect of axial load and bending moment to get the maximum stress on a single pile and comparing this value with the capacity of the pile.

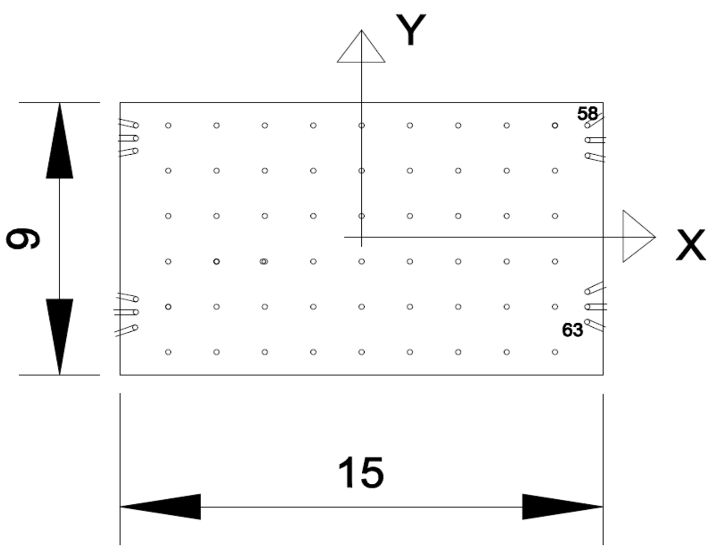

Figure 5.5 Pile cap showing the highly stressed piles

5.3.1 Axial Load on Piles

$$P_{d\max} = \frac{F_{vd}}{n} + \frac{M_{dx} \cdot d_x}{I_y} + \frac{M_{dy} \cdot d_y}{I_x} \tag{5.4}$$

Where:

$P_{d\max}$: Design value of maximum axial load on a single pile

F_{vd} : Factored vertical load acting on the group pile

n : Number of piles

M_{dx} and M_{dy}: Factored bending moment in the X and Y direction

d_x and d_y : Distance from centre of gravity of pile group to pile for which $P_{\max}$ is being calculated

I_x and I_y : Moment of inertia in the X and Y direction

$$I_x = \sum_{i=1}^{n} d_{yi}^{\;2} \quad \text{and} \quad I_y = \sum_{i=1}^{n} d_{xi}^{\;2} \tag{5.5}$$

Substituting the values of d_{yi} and d_{xi} into equation 5.2 we get:

I_x = 1398 m^2 and I_y = 467 m^2

5.3.2 Design Capacity of Piles

First, let’s calculate the maximum design capacity of the wood pile.

The design value X_d of a strength property according to Eurocode 5 version EN 1995-1-1:2004 (E) is given as

$$X_d = k_{\text{mod}} \cdot \frac{X_k}{\gamma_M} \tag{5.6}$$

Where:

X_k is the characteristic value of strength property of timber (Table 3.1)

γ_M is the partial factor for a material property

k_{mod} is a modification factor taking into account the effect of the duration of load and moisture content

According to Eurocode 5 version EN 1995-1-1:2004 (E) the modification factor for solid timber which is subjected to long term action is 0.55 and the partial factor is 1.3.

$$X_d = 0.55 \cdot \frac{35}{1.3} = 14.81 Mpa$$

5.3.3 Stress on pile 58 and 63 when the screen is closed

When the screen is closed, the horizontal force in the Y direction and the resulting moment in the X axis will be considered. Hence, the maximum axial load applied on Pile 58 which is located 7 m in the X direction and 3.75 m in the Y direction can be calculated by inserting all the known values into equation 5.1.

$$P_{d\max 58} = \frac{8928}{66} + \frac{1862 \cdot 7}{467} + \frac{9438 \cdot 3.75}{1398} = 188 kN$$

Similarly, for Pile 63 which is located 7 m in the X direction and -3.75 m in the Y direction.

$$P_{d\max 63} = \frac{8928}{66} - \frac{1862 \cdot 7}{467} + \frac{9438 \cdot 3.75}{1398} = 133 kN$$

The next step is to obtain the maximum moment on pile 58 and 63 due to the lateral load. The maximum moment on pile 58 is 2.36 kNm and on pile 63 2.38 kNm. These values are shown on Figure 5.6 and Figure 5.7 respectively.

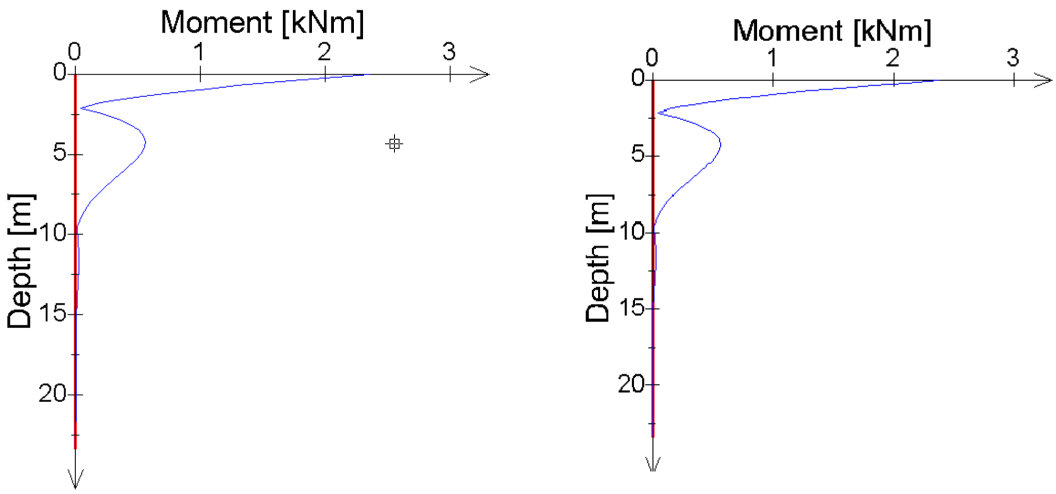

(a) (b)

Figure 5.6 Moments on Pile 58 (a) and Pile 63 (b) when the screen is closed

The maximum axial stress in any pile is given by the following formula.

$$\sigma_{\max} = \frac{P_{d\max}}{A_{pile}} + \frac{M_{pile}}{W} \tag{5.7}$$

Where:

W is moment of inertia of the pile and is give by

$$W = \frac{\Pi \cdot d^3}{32} \tag{5.8}$$

$$W = \frac{\Pi \cdot 0.18^3}{32} = 5.53 \cdot 10^{-4} m^3$$

Substituting all the known values into equation (5.7), we can get the maximum stress on pile 58 and pile 63.

$$\sigma_{\max 58} = \left[\frac{188}{0.025} + \frac{2.36}{5.53 \cdot 10^{-4}}\right] kPa = 11.64 MPa$$

$$\sigma_{\max 63} = \left[\frac{133}{0.025} + \frac{2.38}{5.53 \cdot 10^{-4}}\right] kPa = 9.62 MPa$$

Comparing the maximum stress with the capacity of the pile 14.81 MPa, on both pile 58 and 63 the maximum stresses do not exceed the capacity of the pile. As mentioned above, since pile 58 and 63 are highly stressed piles all the other piles should also be safe.

5.3.4 Stress on pile 58 and 63 when the screen is open

When the screen is open the horizontal force acting in the direction of Y and the associated moment disappear. Hence, the maximum stress according to equation (5.4) can be calculated as.

$$P_{d \max 58} = \frac{8928}{66} + \frac{9438 \cdot 3.75}{1398} = 161 kN$$

$$P_{d \max 63} = \frac{8928}{66} + \frac{9438 \cdot 3.75}{1398} = 161 kN$$

The maximum moment applied on pile 58 and pile 63 when the screen is open is 2.15 kNm and 3.43 kNm respectively. The values are shown in the figures below.

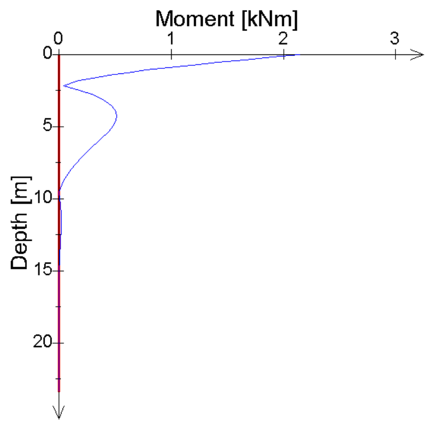

(a)

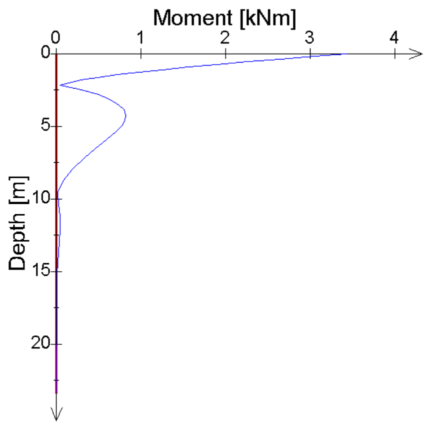

(b)

Figure 5.7 Moments on Pile 58 (a) and Pile 63 (b) when the screen is open

Substituting all the known values into equation (5.7), we can get the maximum stress on pile 58 and pile 63.

$$\sigma_{\max 58} = \left[\frac{161}{0.025} + \frac{2.15}{5.53 \cdot 10^{-4}}\right] kPa = 10.33 MPa$$

$$\sigma_{\max 63} = \left[\frac{161}{0.025} + \frac{3.43}{5.53 \cdot 10^{-4}}\right] kPa = 12.64 MPa$$

In the same manner, the calculation above shows that the maximum stresses are less than the capacity of the piles therefore, the piles are safe against structural failure.

5.4 Ultimate limit state Analysis for Stress in Soil Using Case B

In the ultimate limit state analysis, the maximum utilization of the soil and pile will be checked, moreover the maximum stress in the soil will be checked against the capacity of the soil as shown in the P-Y curve and finally the deflection of the pile will be analysed.

In this problem, pile No. 63 is the most deflected pile of all piles in both cases (when the screen is open or closed) therefore, according to Winkler's spring model the soil around this pile is also the most stressed soil, hence by finding this stress and comparing it with the resistance of the soil as shown in Figure 5.3 we can check if the soil provides adequate lateral support or not.

Table 5.5 Maximum utilization of soil and pile Case B

	Maximum Utilization Screen Closed	Maximum Utilization Screen open	Load (no)[1]	Load step (no)[2] open(closed)	Pile
Axial compression	0.34	0.29	1	2(1)	58
Axial tension	0.26	0.23	1	4(1)	59
Pile stress	0.18	0.25	1	2(1)	63

The maximum utilization of the soil and all the piles in the group is well below 1, and hence it shows that the pile soil interaction can take more loads.

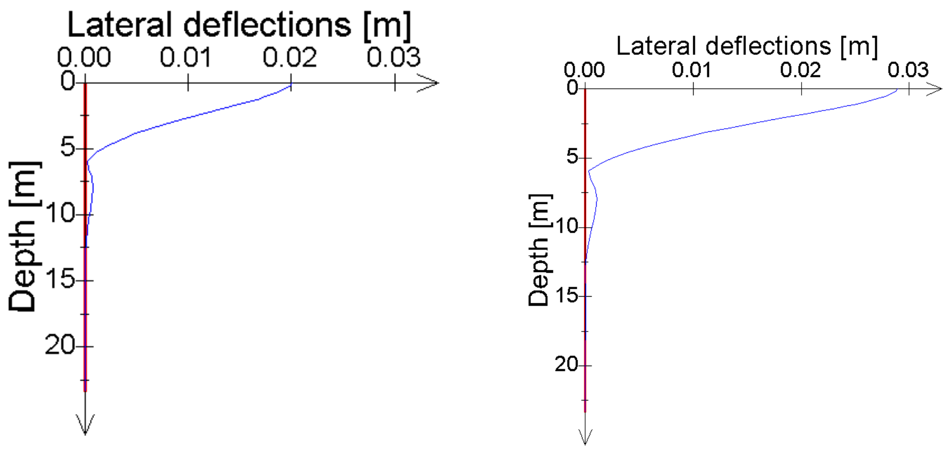

(a) (b)

Figure 5.8 Lateral deflections on Pile No.63 for Case B (a) screen closed and (b) screen open

[1] In Geosuite pile group there is a possibility of inputting different load sets at a time and the program gives results for each load case. In this analysis only one load set is used

[2] The load applied to the structure is in steps. In this case ten load steps is chosen.

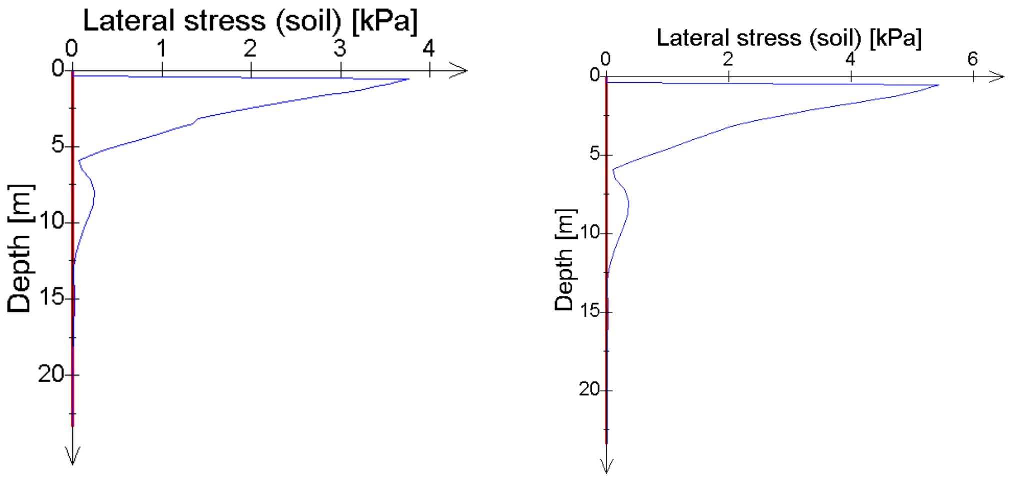

(a) (b)

Figure 5.9 Lateral Stress in the soil around Pile No.63 Case B (a) screen closed and (b) screen open

As shown in the above figure the maximum lateral stress in soil around the pile is 5.4 kPa but the capacity of the soil when the pile deflect by 29 mm as shown in Figure 5.3 is close to 65 kPa, which is much larger than the stress in the soil.

5.5 Ultimate limit state Analysis for Stress in Soil Using Case C

In this case, the lateral soil resistance is reduced due to the application of factor of safety which can be seen in Figure 5.4, for 26 mm deflection of pile the resistance of the soil is approximately 45 kPa. Similarly, the stress in the soil, which is equal to 5 kPa, is very small when compared to the capacity of the soil.

Table 5.6 Maximum utilization of soil and pile Case C

	Maximum Utilization Screen Closed	Maximum Utilization Screen Open	Load (no)	Load step (no) Closed (Open)	Pile Closed (Open)
Axial compression	0.3	0.27	01	1(2)	63(58)
Axial tension	0.23	0.2	01	1(2)	56(59)
Pile stress	0.16	0.23	01	1(1)	63(63)

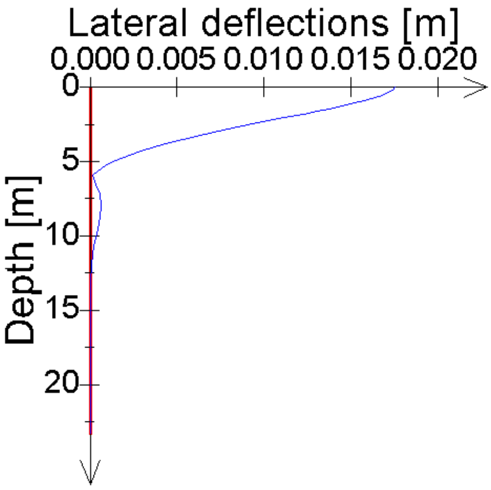

(a)

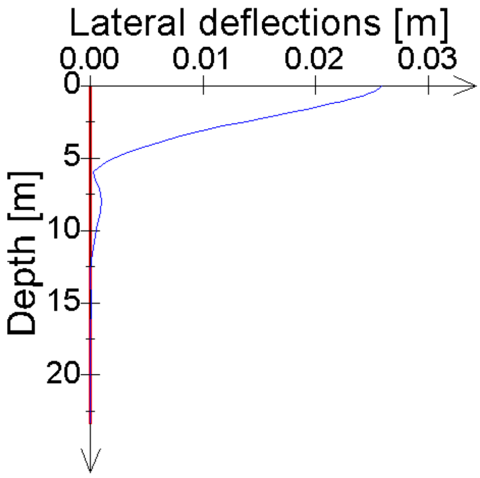

(b)

Figure 5.10 Lateral deflections on Pile No.63 Case C (a) screen closed and (b) screen open

As in Case B, the maximum deflection is occurred on pile No.63.

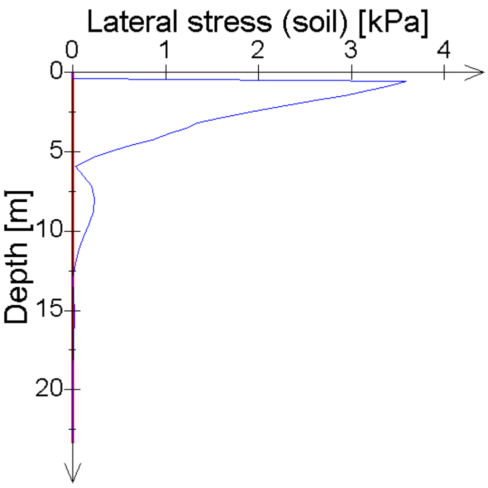

(a)

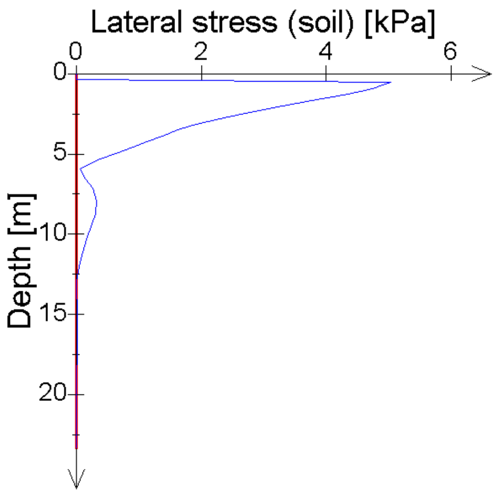

(b)

Figure 5.11 Lateral Stress in the soil around Pile No.63 Case C (a) screen closed and (b) screen open

5.6 Serviceability Limit State Analysis

Serviceability limit state basically concerned with the function of the structure, the structure which is subjected to routing loading must serve the intended purpose, and consequently the deflection should not exceed the maximum limit laid down in the building codes.

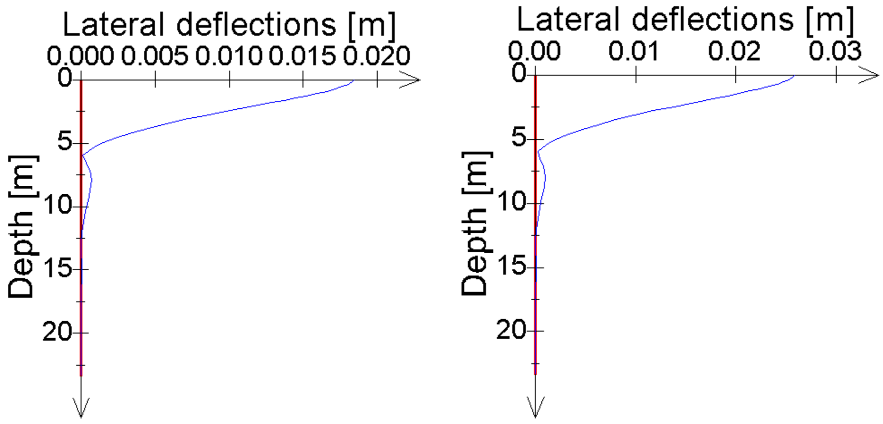

(a) (b)

Figure 5.12 Lateral deflections of Pile No.63 for serviceability limit state (a) screen closed and (b) screen open

As presented in the figure above the maximum lateral defection in the serviceability limit state case is 26 mm. This much deflection can be considered as small enough not to disrupt the function of the structure moreover, since the deflection in the ultimate limit state case is larger than this value it is already assured that the deflection for serviceability state do not cause failure of the soil.

6 Conclusion

The stability analysis of Ormo tower undertaken in this project can be considered as conservative both in terms of calculation of action effect and the corresponding resisting forces however, the unavailability of geotechnical investigation data specifically for this project forced us to use local knowledge available. This might cause some discrepancy in soil strength parameters.

The condition of the wooden pile is also not clearly known; obviously since the piles were installed a long time ago some sort of deterioration might be there which potentially reduce the strength of the pile.

There was one shortcoming in using Geosuite pile group. It was not possible to apply large vertical loads due to convergence problem; therefore hand calculation was necessary to calculate the maximum stresses on the piles. Since the vertical force is not directly used in the Geosuite, second order moment is not considered. This resulted in ignoring the deflection caused by second order moment. Hence, the deflection found in the last section could be a bit higher.

The maximum stress on some of the highly stressed piles, like Pile 58 and Pile 63 is less than the structural capacity of the piles. This shows that the pile group can take more loads. Moreover, the wind load which blows for a relatively shorter time has fewer tendencies to cause structural failure unless it is extremely high.

Finally, the stability analysis performed in the last chapter show that the pile foundation is safe against higher lateral load which anticipated to happen in the future due to change in climate.

7 References

Bowles, Joseph E. (1997): *Foundation Analysis and Design (fifth edition),* The McGraw-Hill Companies, Inc. {Singapore}, 1230pp.

B. Mutlu Sumer, Klavs Bundgaard and Jørgen Fredsøe (2005): Global and local Scour at Pile Groups. International Offshore and Polar Engineering Conference, Seoul, Korea, June 19-24, 2005

DIN 4085 (2007): *Baugrund – Berechnung des Erddrucks* (Sub Soil Calculation of Earth Pressure), German Institute for Standardization, Berlin, October 2007

Eurocode 1: Action on Structures – Part 1-4: General actions- Wind actions, EN 1991-1-4:2005: E

Eurocode 5: Design of timber Structure – Part 1-2: General – Structural fire design, EN 1995-1-1:2004 (E)

Forsberg, B., Messing, M. L., Jakobsson, B. (2002): {(Ormo skärmanläggning FÖRDJUPAD DAMMSÄKERHETSUTVÄRDERING)}, SwedPower AB, {P1279200}, Göteborg, {Sweden}, 124pp.

Geoffrey, Meyerhof G. (1994) Evolution of Safety factors and Geotechnical limit state design The Second Spencer J. Buchanan Lecture November 4, 1994

Gunaratne, Manjriker. (2006): *The Foundation Engineering Hand book,* Taylor & Francis Group. {United States of America}, 625pp.

Li, Y., Chen, X., Fan, S., Briaud, J.L., and Chen, H.C (2009): Is Scour important for Pile Foundation Design in Deepwater? *Offshore Technology Conference in Houston, Texas, USA, 4-7 May 2009.*

Iowa State University (2009, June 26): Climate Change: Some Winds Decreasing Across United States. *ScienceDaily*. Retrieved February, 2010.

Keith F. Faherty and Thomas G. Williamson (1999): *Wood Engineering and Construction Handbook (3rd edition),* The McGraw-Hill Companies, Inc {New York}

Mohammad Salim, J. Sterling Jones (1996): Scour around Exposed Pile Foundation, American Society of civil Engineers, North American water and environment congress, June, 1996.

Sharma, Hari Ram (1973): Bed Load Transport in Open and Closed System, River and Harbour Laboratory, Technical University of Norway, Trondheim, Report No. 600830, January 1973.

Sjöberg, J. (2001): {(Stabilitetsanalys – Ormo Skärmanläggning)}, SwedPower AB, {1415600}, Göteborg, {Sweden}, 5pp.

Swedish Standard Institute (2005): Eurokod 7: Dimensionering av Geokonstruktioner (Eurocode 7: Geotechnical Design), SIS, March, 2005

Trevor L. L. Orr (2006): Development and Implementation of Eurocode 7 *TAIPEI2006 International Symposium on New Generation Design Codes for Geotechnical Engineering Practice,* Taipei, Taiwan Trinity College, Dublin University, Dublin, Ireland, Nov. 2~3, 2006

Unified Facilities Criteria (2004): Deep Foundation: Department of Defense, United States of America.

Appendixes

Appendix I - Site map showing boreholes for CPT tests

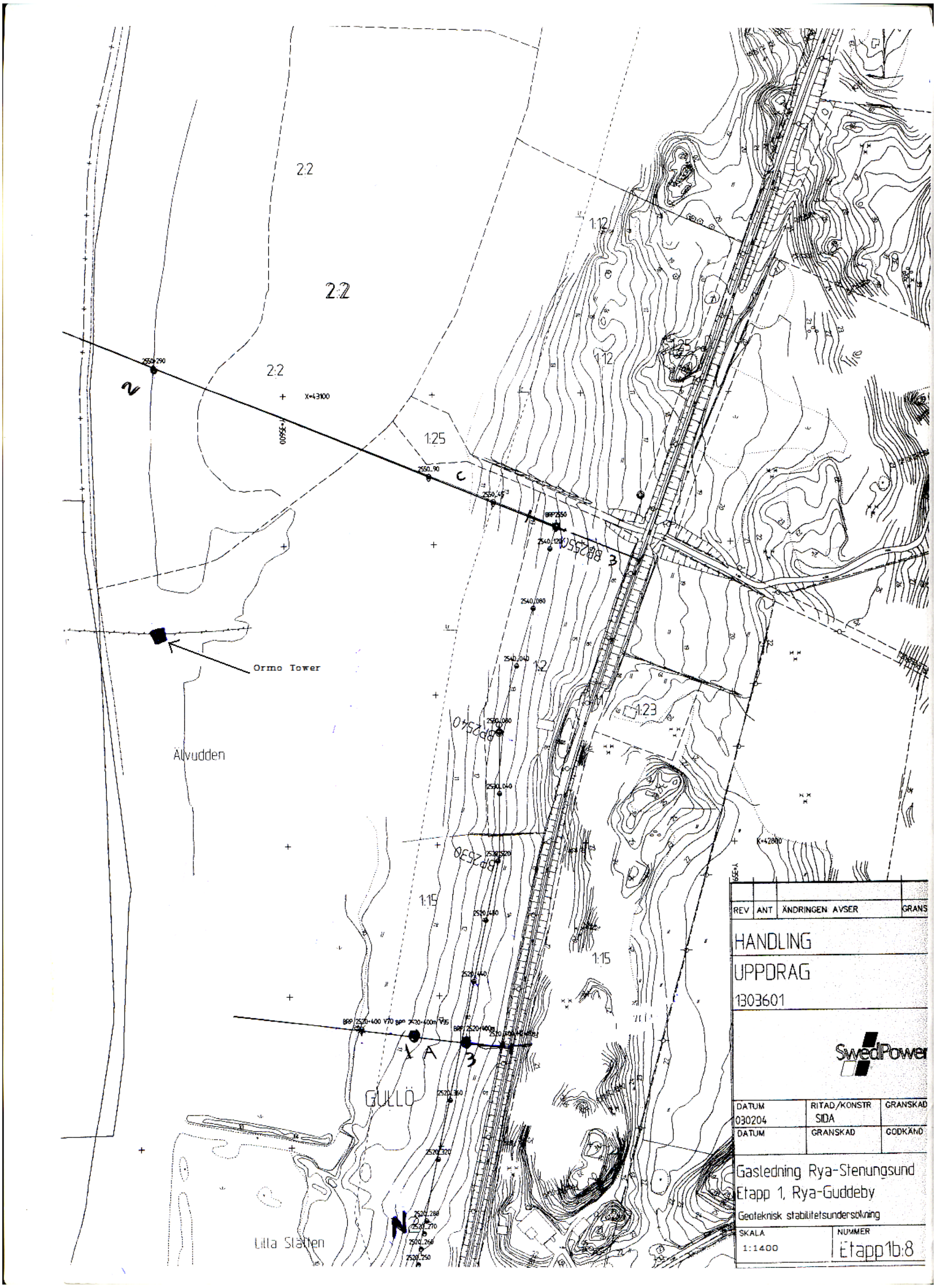

Appendix II - Site map showing boreholes for CPT tests (Continued)

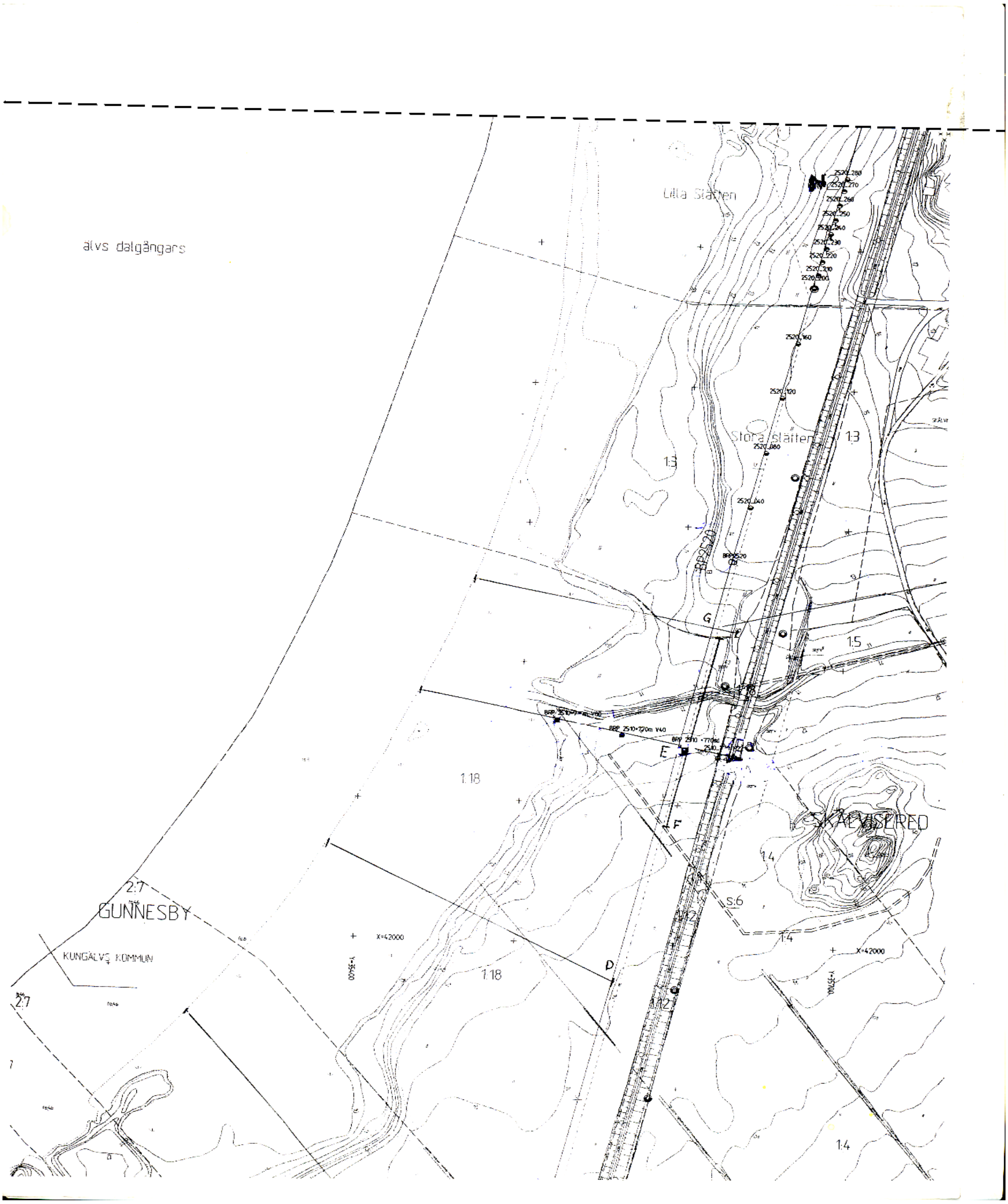

Appendix III – Strength Properties of soft wood

		Poplar and softwood species												Hardwood species					
		C14	C16	C18	C20	C22	C24	C27	C30	C35	C40	C45	C50	D30	D35	D40	D50	D60	D70
Strength properties (in N/mm²)																			
Bending	$f_{m,k}$	14	16	18	20	22	24	27	30	35	40	45	50	30	35	40	50	60	70
Tension parallel	$f_{t,0,k}$	8	10	11	12	13	14	16	18	21	24	27	30	18	21	24	30	36	42
Tension perpendicular	$f_{t,90,k}$	0,4	0,5	0,5	0,5	0,5	0,5	0,6	0,6	0,6	0,6	0,6	0,6	0,6	0,6	0,6	0,6	0,6	0,6
Compression parallel	$f_{c,0,k}$	16	17	18	19	20	21	22	23	25	26	27	29	23	25	26	29	32	34
Compression perpendicular	$f_{c,90,k}$	2,0	2,2	2,2	2,3	2,4	2,5	2,6	2,7	2,8	2,9	3,1	3,2	8,0	8,4	8,8	9.7	10,5	13,5
Shear	$f_{v,k}$	1,7	1,8	2,0	2,2	2,4	2,5	2,8	3,0	3,4	3,8	3,8	3,8	3,0	3,4	3,8	4,6	5,3	6,0
Stiffness properties (in kN/mm²)																			
Mean modulus of elasticity parallel	$E_{0,mean}$	7	8	9	9,5	10	11	11,5	12	13	14	15	16	10	10	11	14	17	20
5% modulus of elasticity parallel	$E_{0,05}$	4,7	5,4	6,0	6,4	6,7	7,4	7.7	8,0	8,7	9,4	10,0	10,7	8,0	8,7	9,4	11,8	14,3	16,8
Mean modulus of elasticity perpendicular	$E_{90,mean}$	0,23	0,27	0,30	0,32	0,33	0,37	0,38	0,40	0,43	0,47	0,50	0,53	0,64	0,69	0,75	0,93	1.13	1,33
Mean shear modulus	G_{mean}	0,44	0,5	0,56	0,59	0,63	0,69	0,72	0,75	0,81	0,88	0,94	1,00	0,60	0,65	0,70	0,88	1,06	1,25
Density (in kg/m³)																			
Density	ρ_k	290	310	320	330	340	350	370	380	400	420	440	460	530	560	590	650	700	900
Mean density	ρ_{mean}	350	370	380	390	410	420	450	460	480	500	520	550	640	670	700	780	840	1080

NOTE a Values given above for tension strength, compression strength, shear strength, 5% modulus of elasticity, mean modulus of elasticity perpendicular to grain and mean shear modulus, have been calculated using the equations given in annex A

b The tabulated properties are compatible with timber at a moisture content consistent with a temperature of 20°C and a relative humidity of 65%

c Timber conforming to classes C45 and C50 may not be readily available.

Appendix IV – CPT test for borehole 2550 V45m

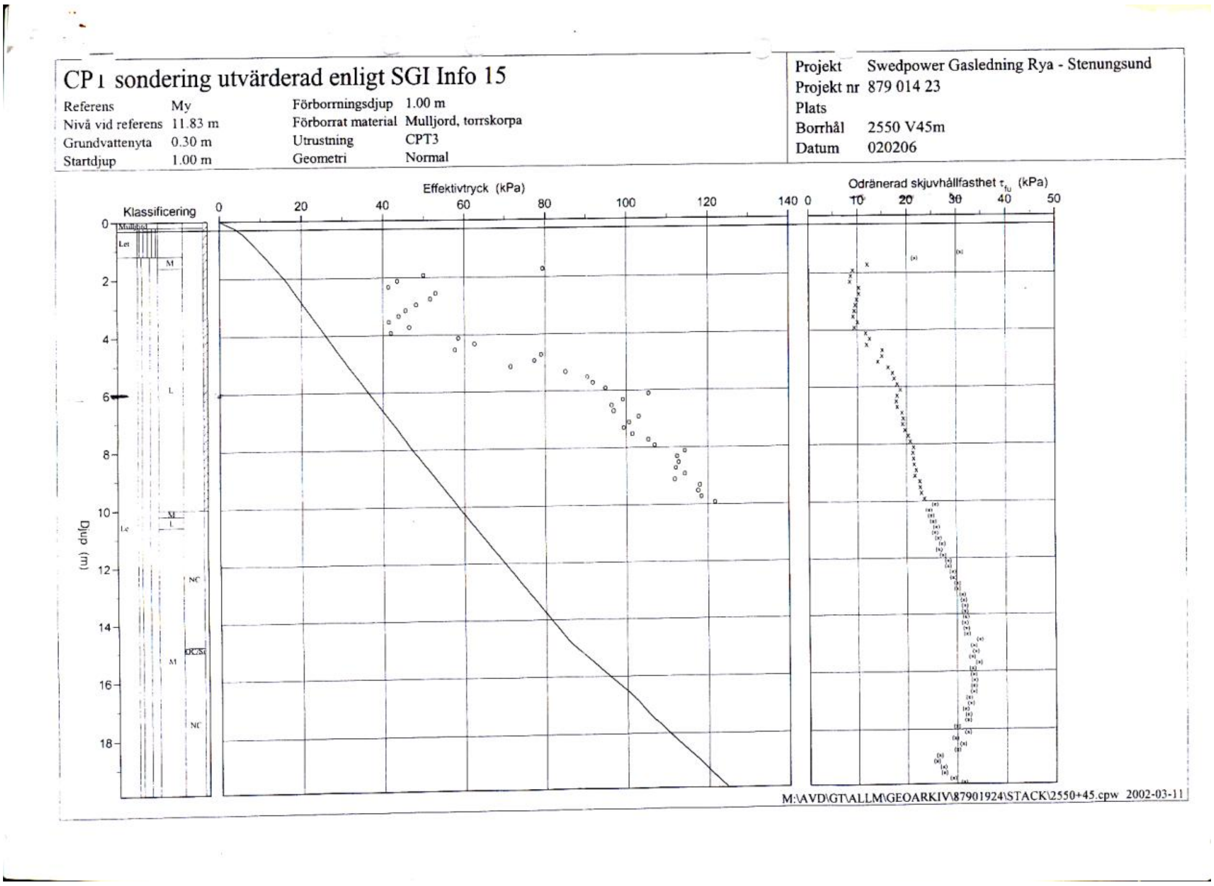

Appendix V – CPT test for borehole 2550 V90m

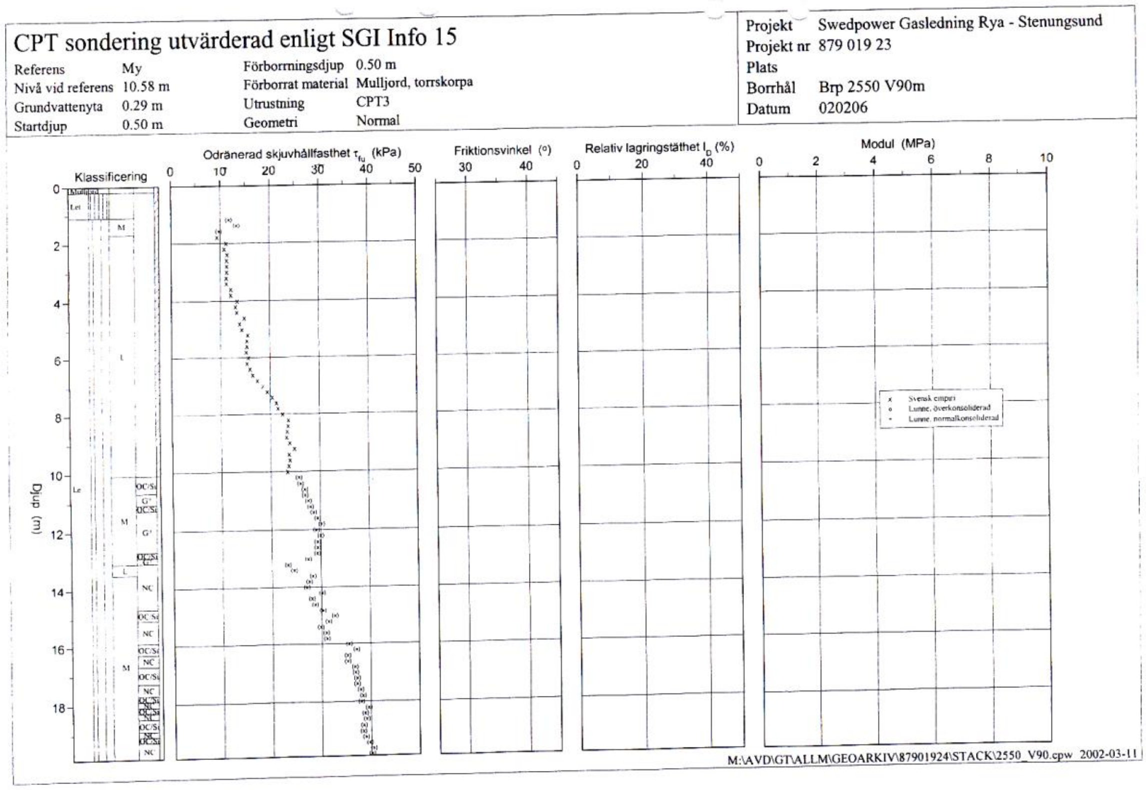

Appendix VI – CPT test for borehole 2550 +250m

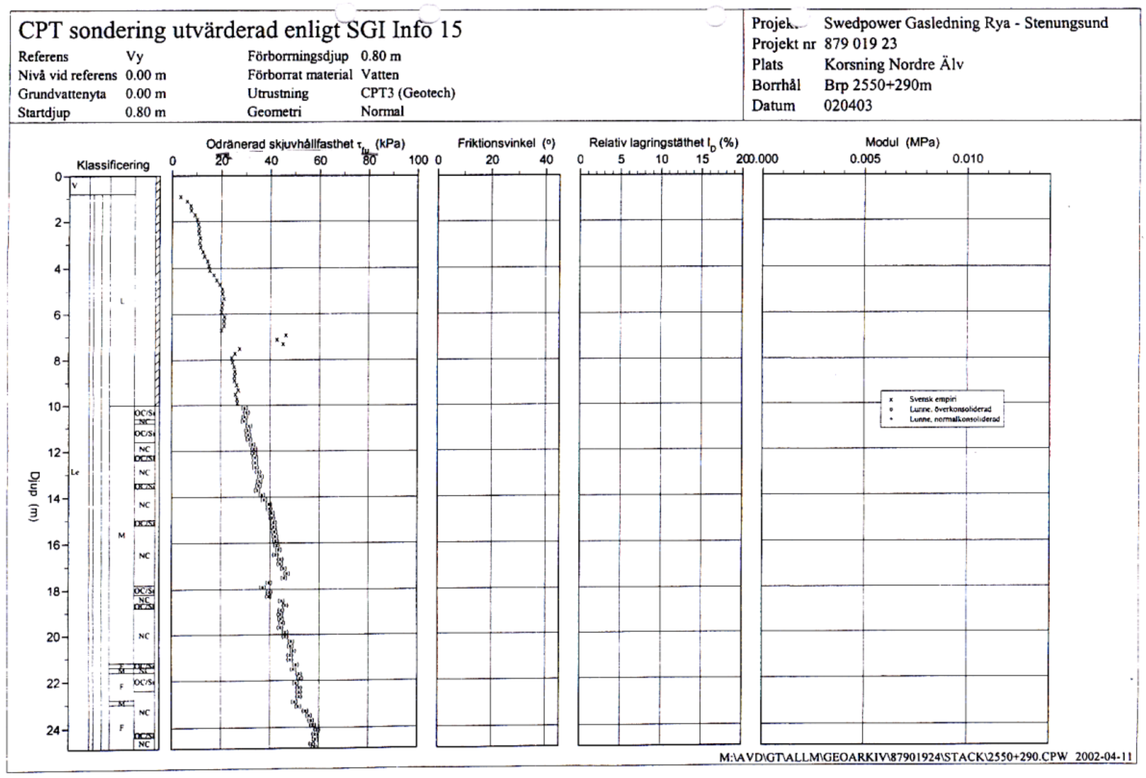

Appendix VII – P-Y curve for Case B and Case C

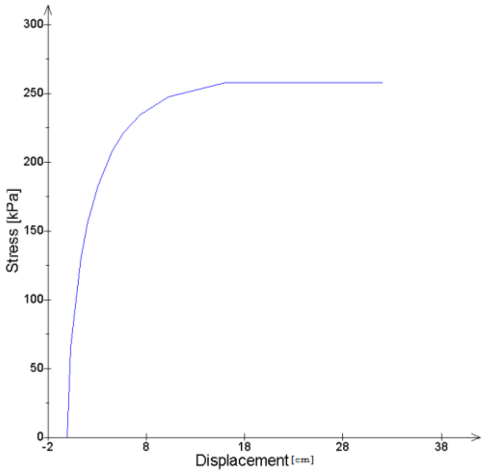

Case B at depth 2.1m

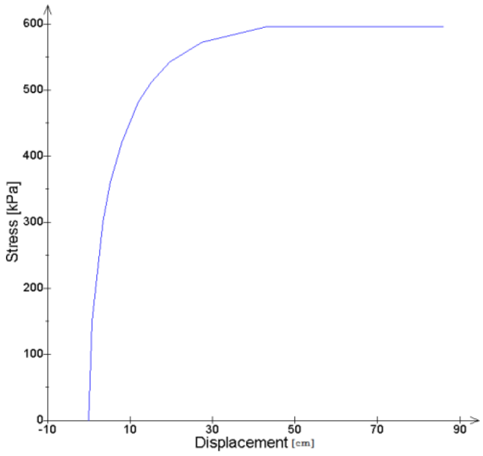

Case B at depth 3.06m

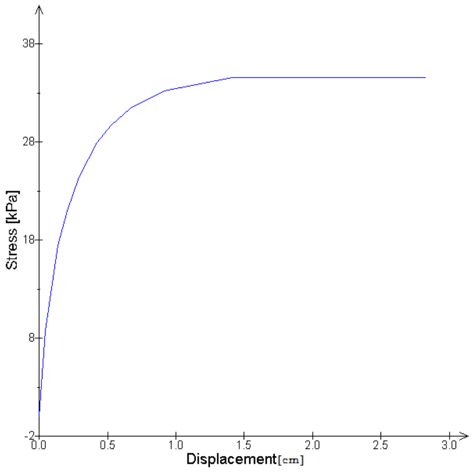

Case C at depth 2.1 m

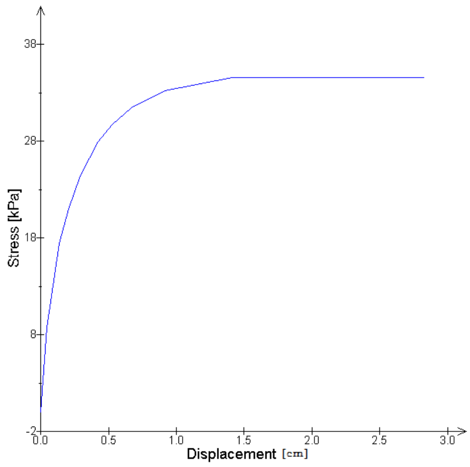

Case C at depth 0.81m